

Presence of clay minerals can obscure spectral evidence of Mg sulfates: implications for orbital observations of Mars

Rachel Y. Sheppard^{a,*}, Ralph E. Milliken^b, Kevin M. Robertson^b

^a Jet Propulsion Laboratory, California Institute of Technology, Pasadena, CA, United States of America

^b Department of Earth, Environmental, and Planetary Sciences, Brown University, Providence, RI, United States of America

ARTICLE INFO

Keywords:

Mg sulfate
clay minerals
Mars
Spectroscopy
hydration state

ABSTRACT

The martian crust is often viewed through the lens of its dominant secondary minerals, Noachian phyllosilicates and Hesperian sulfates, based on orbital spectral observations. However, the effects of surface exposure on the spectra of these hydrous minerals are not fully understood. We use an environmental chamber to measure changes in near-infrared (NIR) spectral absorptions related to H₂O in smectite (montmorillonite) and Mg-sulfate under different temperature, pressure, and relative humidity conditions with relevance to the surface of Mars. Observed spectral differences are attributed to changes in water content (hydration state), mineral phase, and degree of crystallinity. It is observed that even minor changes in hydration state and phase (for Mg sulfate) cause perceptible changes in NIR H₂O absorption features when measured in a controlled laboratory setting under dry Mars-like conditions. Based on these results and the known ability of smectite to rehydrate under increased RH, smectites exposed at the surface of Mars are expected to exchange water with the martian atmosphere under specific conditions, making them active participants in the present-day hydrological cycle of Mars, and in theory these hydration-dehydration processes should be detectable using NIR reflectance spectroscopy. However, some of the spectral changes associated with these hydration changes are subtle and may not be detectable with orbital or landed VNIR spectrometers. Furthermore, we find that the presence of clay minerals can spectrally mask the presence of Mg sulfates under a range of hydration states if the clay minerals are above ~10 wt% abundance. Random noise was added to the laboratory spectral data to simulate orbital-quality reflectance data, and it is observed that expected changes related to hydration state and crystallinity are likely difficult to detect in current orbital VNIR data such as CRISM and OMEGA. This highlights the importance of future *in situ* NIR reflectance observations to accurately determine the extent to which hydrous minerals exposed as the surface cycle water with the martian atmosphere under present-day environmental conditions and to properly assess the role of hydrous minerals in the martian water budget.

1. Introduction

1.1. The martian stratigraphic record of water-rock interaction

It has been well documented over the past fifteen years that the martian surface hosts a variety of OH and/or H₂O-bearing minerals, and a purported time-dependent formation of different hydrous minerals on Mars may record a drying out and overall climatic evolution of the planet over several billion years ago (Bibring et al., 2006; Ehlmann et al., 2011). Clay minerals, for example, are commonly found in Noachian-age (>3.5 Ga) terrains whereas sulfate minerals are associated with Hesperian-age (~2–3.5 Ga) terrains (Bibring et al., 2006; Ehlmann et al.,

2008; Carter et al., 2013). The presence of OH and/or H₂O in these and other hydrous minerals give rise to distinct vibrational absorptions at near-infrared (NIR) wavelengths, allowing their detection using orbital or surface-based visible-near infrared (VNIR) reflectance spectrometers (Bibring et al., 2005, 2006; Poulet et al., 2005; Gendrin et al., 2005; Mustard et al., 2008). H₂O can be associated with minerals in several different forms, including adsorbed on surfaces, weakly hydrogen bonded to specific sites (e.g., interlayer sites in smectite minerals), or structurally bound (e.g., H₂O in sulfates such as CaSO₄ · 2H₂O, gypsum). However, changes in environmental conditions can influence the amount of water that is present in these forms, as well as the overall stability of certain hydrous minerals, which in turn can affect spectral

* Corresponding author.

E-mail address: rachel.y.sheppard@jpl.nasa.gov (R.Y. Sheppard).

<https://doi.org/10.1016/j.icarus.2022.115083>

Received 4 November 2021; Received in revised form 11 April 2022; Accepted 6 May 2022

Available online 11 May 2022

0019-1035/© 2022 Elsevier Inc. All rights reserved.

absorption features that are used for remote mineral detection and identification. Specifically, the stability and hydration state of many hydrous minerals can change in response to variations in atmospheric relative humidity (RH), pressure (P), and temperature (T). As such, confirming the presence and/or specific water content of certain hydrous minerals can be used to infer current or past environmental conditions (e.g., RH, T) on Mars as well as provide information about which hydrous minerals may actively exchange water with the modern atmosphere on diurnal or seasonal cycles.

Results from past studies suggest that while dry martian atmospheric conditions are likely to restrict some hydrous minerals to lower water contents compared with their counterparts on Earth, other hydrous minerals are expected to actively exchange H₂O with the atmosphere over measurable timescales (Beck et al., 2010). As such, hydrous materials in the martian regolith and uppermost crust constitute a meaningful volatile reservoir that may interact with and/or buffer water reservoirs in the near-surface atmosphere and subsurface (Jakosky and Jones, 1997; Bish et al., 2003; Mustard et al., 2008; Pommerol et al., 2009). In addition, certain salts can exist in a variety of hydration states that are highly sensitive to changes in relative humidity (e.g., perchlorates and the MgSO₄ · nH₂O family of minerals). Because of this sensitivity, the confirmed presence of certain hydrous phases may record important information about current or paleo-environmental conditions, including past exposure to high RH conditions (e.g., contact with water ice). If sulfate-bearing strata on Mars record a shift to a drier, more oxidizing climate (e.g., Bibring et al., 2006; McLennan et al., 2018), then understanding the likely hydration state, detection limits, and near-surface stability of different sulfates is critical for understanding the degree to which specific sulfate types or water content are reliable indicators of ancient versus modern processes and conditions.

These potential applications highlight the importance of understanding how changes in the water content of hydrous minerals influence VNIR reflectance spectra and whether or not such changes are likely to be observed in spectral data acquired by previous, current, and future Mars missions. Despite VNIR reflectance spectroscopy being the primary orbital remote sensing technique used to detect sulfate, clay, and other hydrous minerals on Mars, and though a number of previous studies have examined the stability of hydrous minerals under variable T, P, and RH conditions, very few studies have documented the VNIR reflectance properties of such minerals *in situ* under the very dry conditions that typify much of the martian surface. In order to improve our interpretations of the type and water content of hydrous minerals on Mars, and whether or not we should expect to detect changes in these properties over diurnal or seasonal cycles using orbital NIR data, additional laboratory measurements of hydrous minerals under Mars-relevant conditions are needed.

To help fill this gap, we present VNIR reflectance spectra acquired *in situ* of Mg-sulfate and smectite (montmorillonite) samples exposed to a range of conditions designed to induce dehydration, including very low RH conditions experienced by clay and sulfate deposits in Gale crater at various times in the course of a martian year. By starting with materials under ‘wet’ terrestrial conditions (~50–75%RH) and inducing dehydration, we explore the likely range in the strength of water-related absorptions that may be observed in VNIR reflectance data of smectite and Mg-sulfate on Mars. We also examine the degree to which water absorptions under these conditions may spectrally mask the presence of one of these phases when they are intimately mixed. Finally, changes in water absorption strength as measured in high signal laboratory data are evaluated in the context of whether or not similar spectral changes could be reliably identified in lower signal-to-noise orbiter, lander, or rover VNIR data.

2. Background

2.1. H₂O in hydrous minerals

The way in which H₂O is bonded to or within a mineral (i.e., the bond type, strength, and location relative to crystal structure) can be complex and will influence how the mineral responds to changes in T and %RH. In this study, we broadly categorize H₂O associated with hydrous minerals in three ways: surface adsorbed, structurally adsorbed, or structurally bound. The term ‘surface’ adsorbed is used to describe H₂O that is weakly attached to grain/particle surfaces, the abundance of which is therefore influenced by the surface area to volume ratio, i.e., particle size. However, in a number of hydrous minerals there are other factors (e.g., charge imbalance) that result in water being preferentially attached to surfaces unique to the mineral structure. Smectites and zeolites, for example, allow H₂O to be stored in interlayer and channels sites, respectively, which we refer to as ‘structurally’ adsorbed. The amount of water in these sites may be much greater than the amount adsorbed onto the external surfaces of zeolite and clay grains, and both types of adsorbed water may respond to changes in RH on short time-scales (e.g., minutes to hours).

In contrast, structurally bound H₂O is coordinated with a mineral’s crystal lattice and is an integral part of the crystal structure. In many hydrous minerals, this is a stronger bond. Therefore, removing this water requires more energy (e.g., heating) than for adsorbed water. However, in other hydrous minerals, the bonding environment may be weak, and H₂O may be readily lost by decreasing RH (e.g., H₂O in highly hydrated forms of MgSO₄ · nH₂O). The removal or addition of this H₂O represents a reconstructive phase transition and occurs in a number of hydrous salts. In the context of Mars, certain minerals with structurally bound H₂O are predicted to retain water at Mars-like conditions and may represent H₂O ‘sinks,’ including some Mg and Ca sulfates (Vaniman et al., 2004; Robertson and Bish, 2013). In contrast, minerals that more readily exchange H₂O (e.g., smectites) may play a more active role in exchanging water with the modern atmosphere (see Fialips et al., 2005 for a thermodynamics-based discussion of this issue).

We examined two of the most common hydrous mineral types that have been identified on Mars using orbital VNIR reflectance spectroscopy and that also span a range in structurally adsorbed versus structurally bound H₂O: a smectite (montmorillonite) and hydrous Mg-sulfate. Both mineral classes have been identified on Mars *in situ* (Wang et al., 2006a; Wang et al., 2006b; Grotzinger et al., 2014; Sutter et al., 2017; Bristow et al., 2018; Rapin et al., 2019), and the data presented below are complementary to a number of previous studies that have explored the stability of Mg-sulfate under Mars-relevant conditions, albeit under different T-RH combinations and/or with different analytical methods (e.g., Raman spectroscopy, X-ray diffraction) than presented here. Based on those studies and theoretical considerations, it is expected that smectite and Mg sulfate will exhibit changes in hydration state, and we seek to determine if such changes could take place on timescales relevant to diurnal cycles on Mars (e.g., minutes to hours) and how water loss due to decreasing RH compares with water loss induced by decreasing pressure or increasing temperature. We also assess the degree to which predicted hydration changes may be observed in VNIR reflectance data. Physical mixtures of the two phases were synthesized and examined to better understand how the presence of one phase and its hydration state may influence the detectability of the other phase at VNIR wavelengths. The resulting data allow for direct comparison with reflectance spectra of Mars acquired from orbital instruments such as the Observatoire pour la Mineralogie, l’Eau, les Glaces et l’Activite (OMEGA) and Compact Reconnaissance Imaging Spectrometer for Mars (CRISM), as well as rover-based VNIR spectra acquired by SuperCam on the Perseverance rover.

2.2. Mg sulfates on Mars: Spectral characteristics and stability

In the literature on martian sulfates detected from orbital VNIR data, these minerals are often grouped in terms of the number of structurally bound waters: sulfates with no structural water are anhydrous, sulfates with one structural water are monohydrated, and sulfates with more than one (2 to 11+) water molecules per unit cell are referred to as polyhydrated. VNIR reflectance spectra are sensitive to bonding environments and vibrations associated with H₂O, OH, and SO₄, and can be used to distinguish between these broad groups. Spectra of monohydrated Mg sulfate (i.e., kieserite, MgSO₄ · H₂O, Fig. 1c.) exhibit a strong absorption that starts near ~1.9 μm and has a minimum near 2.1 μm that is often boxy in shape, in conjunction with a weaker and narrower absorption centered near 2.4 μm. The 1.9–2.1 μm feature is caused by H₂O interacting with the sulfate ion (Gendrin et al., 2005), whereas the 2.4 μm feature is caused by SO₄²⁻ stretching vibrations (Cloutis et al., 2006; Mangold et al., 2008; Bishop et al., 2009). Reflectance spectra of polyhydrated Mg sulfate (PHS) (*n*H₂O > 1, Fig. 1 d-e) exhibit a strong H₂O absorption at 1.93–1.95 μm and a strong drop in reflectance at wavelengths >2.3 μm. The drop in reflectance is due to the strength of a broad absorption located near 2.4 μm (Clark et al., 1990; Gendrin et al., 2005; Cloutis et al., 2006; Mangold et al., 2008). Under ambient terrestrial conditions, polyhydrated Mg sulfates are commonly in the form of epsomite (MgSO₄ · 7H₂O) and hexahydrate (MgSO₄ · 6H₂O), (Fig. 1 d-e.) depending on RH.

Both polyhydrated and monohydrated Mg sulfate have been detected on Mars from orbit. Orbital mapping has shown mono- and polyhydrated Mg sulfate to be in close proximity to each other in both Gale crater (Sheppard et al., 2020; Sheppard et al., 2021), home to the Curiosity rover, and deposits within the Valles Marineris (Roach et al.,

2009; Mangold et al., 2008; Murchie et al., 2009). The co-location of these phases is intriguing given that they are presumably exposed to similar pressure, temperature, and RH conditions at the surface. The exposures in Valles Marineris are interpreted as evidence of recent hydration from kieserite to PHS (Roach et al., 2009; Murchie et al., 2009). In Gale crater, the monohydrated Mg sulfate appears to be stratigraphically confined, whereas the PHS appears to occur over a range of stratigraphic levels. Orbital mapping also suggests the presence of PHS at previous locations along the Curiosity rover traverse path, but it was not identified in CheMin X-ray diffraction (XRD) measurements at these locations. If the interpretation of the orbital data is correct, this suggests the PHS may occur as an X-ray amorphous form (Sheppard et al., 2020). These observations highlight the need to understand how water content and crystallinity of Mg sulfate relates to spectral features and whether true mineral forms can be distinguished from hydrous amorphous forms using VNIR spectroscopy.

Experimental work and thermodynamic calculations have shown the Mg sulfate system and phase boundaries therein to be complex, particularly at low temperatures. Kieserite can hydrate to PHS, although the hydration is kinetically slow (Vaniman and Chipera, 2006). PHS can respond relatively quickly to changes in RH, likely recording relatively recent conditions on the surface (Roach et al., 2009; Murchie et al., 2009; Sheppard et al., 2020). PHS can increase in hydration when exposed to elevated RH; however, when exposed to low RH it does not dehydrate to kieserite, but rather to an X-ray amorphous but still polyhydrated (1–2 · H₂O) form. Therefore, a hydrated amorphous form of Mg sulfate, and not kieserite, may be present in deposits that were originally polyhydrated but that have since experienced low RH or cyclical changes in RH, even if the current RH is quite low (Vaniman et al., 2004; Vaniman and Chipera, 2006; Chipera and Vaniman, 2007).

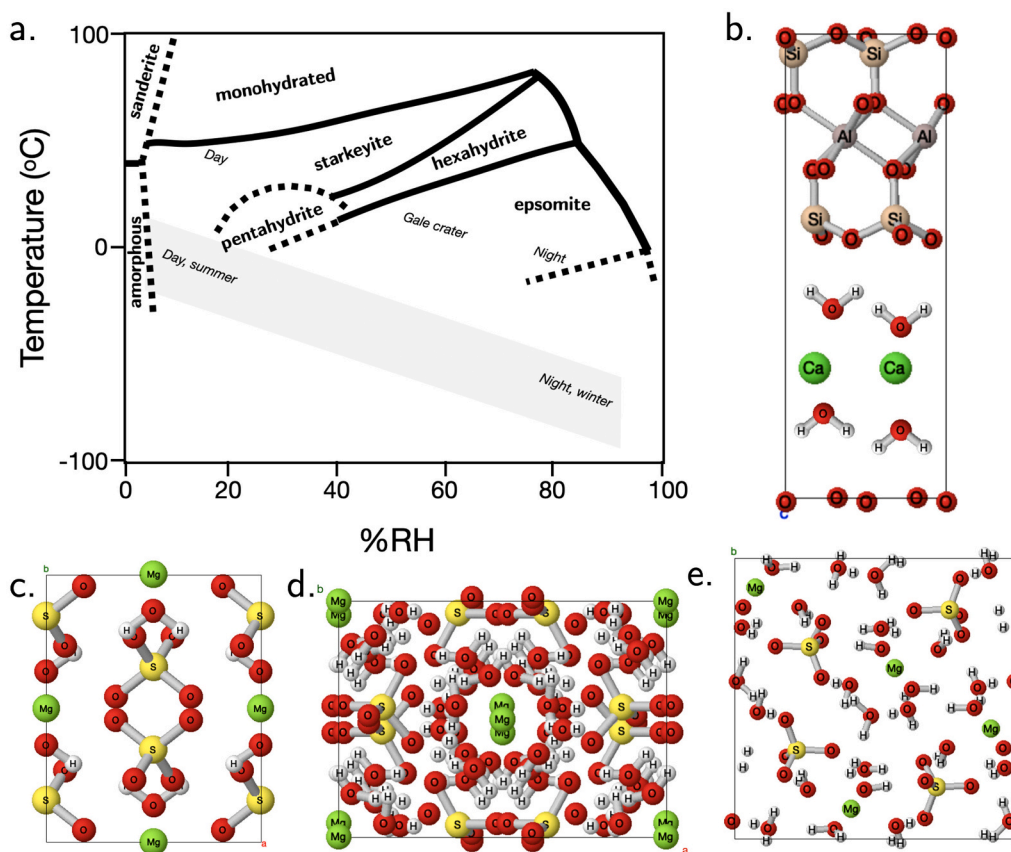


Fig. 1. a. The stability field of Mg sulfate at 0.1 MPa, based on Hogenboom et al., 1995; Chou and Seal, 2003; Chipera and Vaniman, 2007; Chou et al., 2013. Surface %RH and T conditions are based on Savijärvi, 1995 and Martin-Torres et al., 2015. b-e. Mineral structures from Mindat: b. montmorillonite, c. kieserite, d. hexahydrate, e. epsomite.

The $\text{MgSO}_4 \cdot \text{H}_2\text{O}$ phase diagram is characterized by extensive fields of metastability at low temperature conditions. Previous experiments, (Chipera and Vaniman, 2007) show the boundaries between metastable states are approximate with considerable overlap. At low latitudes, including Gale crater, dehydration should be thermodynamically favorable. For such latitudes, lower temperatures would lead to sluggish kinetics that may allow Mg sulfate to be metastable at the surface, coexisting in multiple hydration states (Vaniman et al., 2004; Vaniman and Chipera, 2006; Roach et al., 2009; Wang et al., 2011). *In situ* observations will be necessary to truly understand the relationship among the Mg sulfates and their host rock, and it is currently unclear which forms may be expected to coexist, as well as which are stable over long timescales and thus dominated by seasonal and orbitally-driven cycling of T and RH.

2.3. Smectites on Mars: Distribution and spectral characteristics

Many types of clay minerals have been detected on Mars, but the most widespread are Fe-, Mg-, and Al-rich smectites. Water in the smectite interlayer is relatively weakly bound, particularly H_2O that is hydrogen bonded to other interlayer H_2O molecules rather than bonded to interlayer cations. As such, vibrational absorptions associated with the former will occur close to but at slightly longer wavelengths than the latter; this H-bonded interlayer water is the most easily affected by changes in RH. In contrast, structural OH in smectites and other clay minerals is strongly bonded to the octahedral cations (e.g., primarily Al and Mg in montmorillonite) (Bishop and Pieters, 1995) and the associated spectral features are not expected to be influenced by changes in RH alone. H_2O that is surface or structurally (interlayer) adsorbed to smectite will give rise to near-IR absorptions at 1.4 and 1.9 μm , whereas structurally bound OH will produce combination bend plus stretch vibration absorptions near $\sim 2.2\text{--}2.3 \mu\text{m}$, the exact position of which depends on the octahedral cation(s) (Clark, 1981; Bishop and Pieters, 1995). Specifically, this absorption will exhibit a reflectance minimum at $\sim 2.28 \mu\text{m}$ for Fe-OH (e.g., the Fe^{3+} smectite nontronite), $\sim 2.2 \mu\text{m}$ for Al-OH (e.g., the smectite montmorillonite, Fig. 1b), and $\sim 2.31 \mu\text{m}$ for Mg-OH (e.g., the smectite saponite) (Clark et al., 1990; Bishop et al., 2008).

In clay-bearing regions on Mars, the metal-OH absorption is commonly observed to have a reflectance minimum at 2.29–2.31 μm , consistent with Fe/Mg varieties (Ehlmann et al., 2013; Carter et al., 2013). Significant expanses of Al-bearing clays have also been observed, particularly in the terrain surrounding Mawrth Vallis and plains adjacent to Valles Marineris (Mustard et al., 2008; McKeown et al., 2009; Noe Dobrea et al., 2010; Ehlmann et al., 2013). In terms of hydration, it is well documented that the interlayer cation of smectite exerts a strong control on the H_2O adsorption properties of the interlayer region, and in this study we use a single smectite (montmorillonite) that is widely available and with a well-characterized interlayer cation composition. A Ca-bearing montmorillonite was selected over other smectites (including nontronite) based on its wider laboratory availability and the secondary goal of examining whether the Ca may be mobilized under these conditions to produce any mixed-cation or Ca-bearing sulfates (e.g., Wilson and Bish, 2011, 2012).

2.4. Clay and sulfate detection limits for Mars

The apparent spatial and temporal distribution of clays and sulfates in the martian rock record (e.g., Bibring et al., 2006) raises questions about the detection limits of these phases when they occur together in complex mineral assemblages. Indeed, Milliken et al. (2009) demonstrated that from a chemical weathering and mass balance perspective, clay-rich terrains on Mars should also host or at least be associated with the production of complementary salts (possibly sulfates) if the clays are derived from a basaltic precursor. Though there are exceptions at a local scale, the lack of clay-sulfate assemblages at a global scale raises the

question as to the fate of these now “missing salts” (Milliken et al., 2009). In that study, it was suggested that spectral masking of such salts in OMEGA and CRISM data or detection limits alone could likely not fully explain this conundrum, but quantitative demonstration of spectral masking was beyond the scope of that work.

Subsequently, laboratory studies of clay-sulfate mixtures and application of radiative transfer models (e.g., Hapke-based models) to VNIR spectra of those mixtures has provided some quantitative metrics for assessing sulfate and clay detection in binary systems. Stack and Milliken (2015) presented spectral modeling results for montmorillonite, saponite, and nontronite clays mixed with Mg-sulfate. They found that although the spectra could be reproduced within $\sim 2\%$ using a Hapke-based model, the presence of clays could not be reliably detected when present at abundances $< 10\%$. In contrast, Mg-sulfate abundances as low as 5–10% could be detected in the clay-dominated mixtures. However, the Mg-sulfate in that study was in a highly hydrated form – epsomite and/or hexahydrate – that gives rise to subtle but distinct spectral properties. Such high hydration states are not likely to exist in most regions of the surface of Mars, particularly in near-equatorial zones such as Gale crater. It is more likely that Mg-sulfate may be present in a lower hydration state (e.g., Vaniman et al., 2004; Vaniman and Chipera, 2006; Chipera and Vaniman, 2007), and the spectral characteristics of those forms of hydrous Mg-sulfate may not be as readily detectable.

Additional radiative transfer modeling by Robertson et al. (2016) of spectra for montmorillonite-gypsum mixtures also demonstrated that the two components could be identified and reasonably modeled when present at abundances of 10 wt% or more. But that study also relied on data acquired under ambient conditions and discussed how the strength of the H_2O absorption features can strongly influence model results. In addition, gypsum exhibits diagnostic spectral features that do not overlap with clay (smectite) features as significantly as for Mg-sulfate. Together, these studies highlight the need to acquire spectra of clay-sulfate (and Mg-sulfate in particular) mixtures under Mars-relevant conditions to better understand how more realistic variations in the strength and shape of H_2O features may influence the detection of sulfates in clay-bearing terrains and vice versa.

2.5. Laboratory smectite and sulfate spectra under Mars-relevant conditions

Several previous studies have compared how mineral spectra differ between samples exposed to ambient laboratory and Mars-relevant conditions. Past experiments have studied the effect of lowering temperature and/or pressure on smectite and/or sulfate spectra (Clark, 1981; Bishop and Pieters, 1995; Cloutis et al., 2007; Cloutis et al., 2008; Jamieson et al., 2014; De Angeles et al., 2017; Turenne et al., 2022), and while many of these studies achieved low temperatures ($\sim 230 \text{ K}$) and pressures, %RH was often not varied or tracked. Some recent studies have extended this to include %RH monitoring (Pommerol et al., 2009; Chou et al., 2013; Pitman et al., 2014; Sklute et al., 2018). However, spectra were often measured *ex situ* under ambient conditions where T, P, and RH are higher than the martian surface, allowing the possibility for the mineral to experience phase transition during analysis.

Based on previous X-ray diffraction (XRD) studies, sluggish hydration reaction rates are expected for kieserite in experiments conducted under Mars-like conditions whereas dehydration of epsomite/hexahydrate proceeds much faster (Vaniman et al., 2004; Vaniman and Chipera, 2006; Chipera and Vaniman, 2007). Several other XRD and Raman studies have monitored phase stability through *in situ* observation while controlling RH at low T (e.g., Robertson and Bish, 2013; Wang et al., 2011), but these data do not translate directly into what changes may be observable in orbital VNIR reflectance data acquired by instruments such as CRISM and OMEGA. Indeed, there have been few if any systematic *in situ* VNIR reflectance studies for hydrous minerals under the dry conditions that are common diurnally and/or seasonally for many locations on Mars, particularly at combined low T and low RH

conditions. Laboratory measurements of hydrous minerals under true Mars-like low T and low RH conditions are experimentally difficult due to the extremely small amount of water that must be maintained or controlled in the experimental setup, a persistent challenge on our water rich planet. As a first step in addressing this gap, we present here spectral data for low RH experiments and evaluate how dehydration induced by this method compares with dehydration induced by increasing temperature and decreasing pressure. Ongoing experiments are focused on combined low T and controlled RH conditions, and the cycling of these variables, to understand the dynamic behavior of hydrous minerals under Mars-like environmental conditions and for comparison with the 'dry' endmember scenarios presented here.

3. Methods

3.1. Mineral samples and mixtures

The VNIR spectral properties of powdered Mg sulfate and montmorillonite were studied over the course of 10 experimental runs. The montmorillonite (SAz-2) was purchased from the Clay Minerals Society and has Ca as the dominant interlayer cation, which may influence how the mineral exchanges H₂O with the atmosphere during the experiments (Bishop and Pieters, 1995; Bish et al., 2003). The starting Mg sulfate was a commercially available epsomite (MgSO₄ · 7H₂O). The epsomite was analyzed by powder X-ray diffraction to confirm its mineral purity (Supplemental Information Fig. 1); based on the ambient %RH in the lab, the starting hydration state for the experiments was a mixture of epsomite and hexahydrate (MgSO₄ · 6H₂O). Mineral samples were gently powdered using a corundum mortar and pestle. The Mg sulfate was sieved to a range of 75–125 μm to reduce the variability of surface adsorbed water relative to the total water content of the sample. Three physical mixtures of Mg sulfate and montmorillonite were also synthesized at ratios of 10/90 (10% Mg sulfate, 90% montmorillonite), 50/50 (50% Mg sulfate, 50% montmorillonite), and 90/10 (90% Mg sulfate, 10% montmorillonite). Each mixture was prepared directly before the experiment was begun to limit any changes in hydration state or cation exchange between the phases that might occur under ambient conditions. The proportions were based on mass as measured by a laboratory balance and physical mixing was done by gently shaking the powdered materials in a glass vial.

3.2. Experimental setup

Approximately 5–10 mg of sample was loaded into a small ~2 mm-deep cavity in a copper sample holder. A clean glass slide was used to remove excess sample above the top of the sample cup to create a flat sample surface for analysis. Halon powder was firmly pressed into a second cavity in the copper holder to act as a white reference standard. The copper sample holder was then placed in a Linkam THMS350V environmental chamber and covered with a lid that allowed the sample and reflectance standard to be viewed through a CaF₂ window. Ports on the sides of the chamber allow for attaching a vacuum pump and/or flow-through of externally supplied gases.

Relative humidity is a ratio of the partial pressure of H₂O (p) relative to the saturation partial pressure of H₂O (p_{sat}; calculated with respect to liquid for this study). The latter will vary as a function of temperature; thus, for a fixed p_{H₂O}, the RH will increase with decreasing temperature and vice versa. For the experiments discussed here, dry air with a dew point of -70 °C was generated with a Parker-Balston purge gas generator and verified with a Vaisala low dew point probe. This dewpoint is equivalent to an RH of ~0.016% at ambient temperature and pressure (per the Clausius-Clapeyron equation). The dry air was passed into the Linkam stage through an inflow port and a similar port on the opposite side of the stage was left open to allow the air and any water evolved from the sample to leave the chamber. The interior of the stage was maintained at slight positive pressure to ensure continuous flow of dry

air through the chamber. The copper sample holder was in direct contact with a heating/cooling stage, the temperature of which was controlled using the LinkSys32 software included with the Linkam environment stage. To raise %RH, the sample stage can be cooled to a desired temperature (typically -50 to -68 °C) via automated pumping of liquid nitrogen from a 7 L dewar through the stage (Fig. 2b.). For dehydration experiments that relied on low pressure, an Edwards E2M1.5 rotary vacuum pump was attached to the Linkam stage, as well as a Pfeiffer Pirani gauge to monitor the sample chamber pressure (Fig. 2a.).

3.3. Experimental conditions

Experimental runs were designed to examine possible dehydration behavior at different Mars-relevant conditions. Ambient lab conditions resulted in the starting samples being at a higher hydration state than expected for much of the martian surface, thus a practical result of our analyses was to observe the dehydration of samples to understand changes in VNIR reflectance properties over a range in sample water content. Sample dehydration was induced three ways: via increasing temperature, lowering pressure (i.e., exposure to a ~ 0.016 mbar vacuum), or exposure to low %RH air. Though not expected to occur at the martian surface, elevated temperatures were explored to understand how thermally induced dehydration compares with dehydration induced by lowering P and lowering RH. The pressure that mineral samples were exposed to in the low pressure (vacuum) experiments is notably lower than average annual martian atmospheric pressure of ~6 mbar (Hess et al., 1979), but a primary goal of this step was to induce large changes in hydration solely by pressure to understand the maximum possible VNIR spectral response of the samples under low P conditions. A total of 10 dehydration experiments were conducted (Table 1).

3.4. X-ray diffraction

Powder X-ray diffraction (XRD) measurements were carried out for select samples before and after experimental runs to confirm the mineral phases inferred from the VNIR spectral properties. All XRD patterns were acquired using a Bruker D2 Phaser instrument with a Cu Kα source. XRD patterns were analyzed for presence/absence of relevant peaks based on comparison with patterns in the International Centre for Diffraction Data database. Measurements before experimental runs were taken from 5–90° 2θ at 0.02° 2θ step size, in Bragg-Brentano geometry. After experimental runs, the scan duration and 2θ range were typically decreased to speed up the XRD pattern acquisition in order to minimize the chance of sample rehydration, a process that may occur when the sample was removed from the environmental chamber and re-exposed to ambient lab conditions. In these cases, the 2θ range was chosen to focus on regions where diagnostic clay or sulfate diffraction peaks are expected to occur. No baseline subtraction was performed.

3.5. Measurement and analysis of VNIR reflectance spectra

VNIR reflectance spectra (0.35–2.5 μm) were collected throughout the experiments using an Analytical Spectral Devices (ASD) FieldSpec3 spectroradiometer. Samples were illuminated with a fiber optic cable positioned at an incidence angle of ~30° using a white light (quartz tungsten halogen) source. Spectra were acquired for a ~ 5 mm diameter spot size using a fiber optic cable positioned at an emergence angle of 0°. Spectra were first obtained at ambient laboratory conditions and then at regular intervals once an experiment had begun (e.g., raising or lowering temperature and/or pressure, and/or starting the flow of dry air). Spectra were collected approximately every 2–5 min throughout an experimental run until there were no obvious further changes in the VNIR reflectance properties.

Reflectance spectra were calculated by dividing all spectra of the sample by the spectrum of the pressed Halon standard as measured

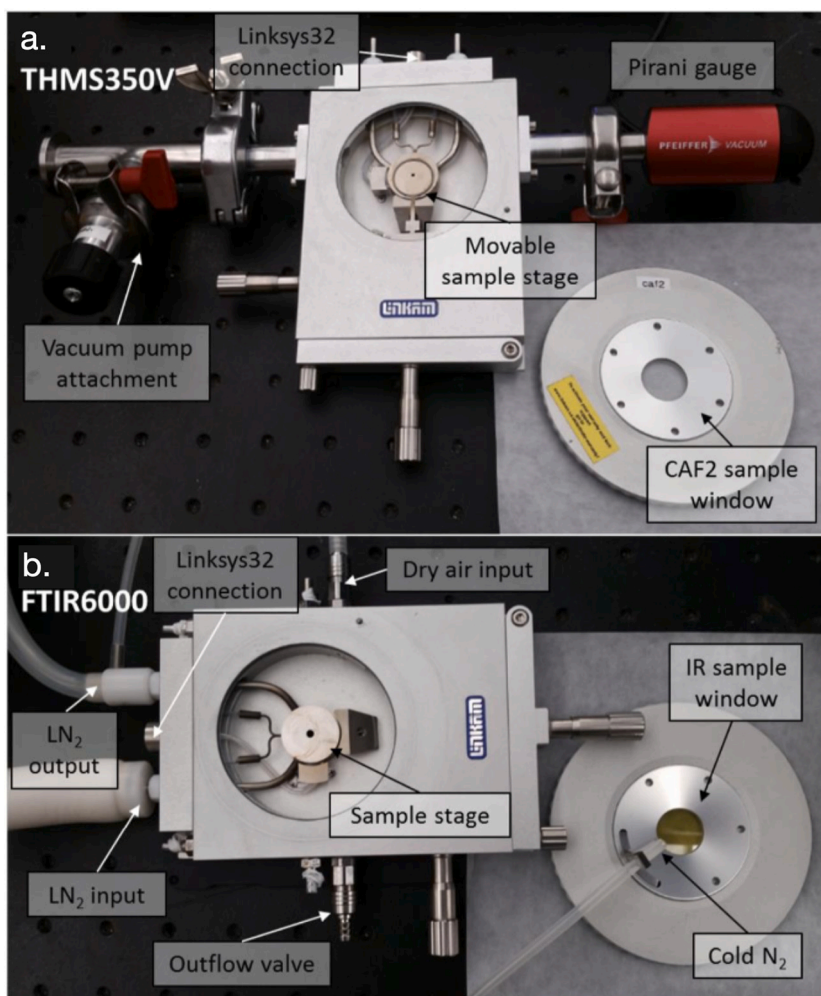


Fig. 2. Experimental setup. a. Low pressure vacuum setup, with attached vacuum pump and Pirani gauge. b. Low temperature high RH setup with LN₂ dewar. Dry air with a dewpoint of -70 °C can be passed through the chamber and removed through an outflow valve. Figure modified from Sun (2016).

Table 1

Parameters for dehydration experiments. The number 626–642 are sample run numbers for reference. MGS: Mg sulfate.

Mineral(s)	Increased T	Low RH (ambient T)	Low P (ambient T)
Montmorillonite	634: 100 °C, 4 h	630: 8 h	633: 3 h
10/90 MGS/mont.	637: 80 °C, 5.5 h	638: 22.5 h	
50/50 MGS/mont.		627: 20 h	
90/10 MGS/mont.		642: 15.5 h	
Mg sulfate	635: 100 °C, 3 h	626: 7 days	632: 2.5 h

under the same viewing geometry and environmental conditions (Supplemental Information Fig. 2). Spectra for some samples exhibited a change in overall reflectance level (albedo), possibly as a result of dehydration causing changes in the height of sample within the sample cup relative to the Halon standard. To correct for this effect, all spectra were scaled to a common reflectance value at a similar wavelength. This scaling step was done by finding the highest reflectance point in the ambient measurement and scaling subsequent spectra to match that point. This allows for more accurate comparison of changes in absorption properties throughout an experimental run (Supplemental Information Fig. 3). Finally, when calculating relevant band depth values, a piecewise linear fit was used to define the spectral continuum for each spectrum and the scaled reflectance spectra were then divided by the continuum and converted to band depth spectra following the method of

Clark and Roush (1984). The resulting continuum-removed spectra are characterized by a value of 0 when there is no absorption present and a value of 1 when an absorption is completely saturated. All band depth values (Clark and Roush, 1984), positions, and shapes discussed below were assessed using the processed continuum-removed data. In this study we focus on absorption features related to OH and H₂O, as discussed above, to assess how T, P, and RH influence the apparent hydration state of the samples at VNIR wavelengths. These spectra cover a similar wavelength range as the OMEGA and CRISM instruments that have been used to identify hydrous minerals on Mars and also allow for comparison with previous laboratory VNIR data of Mg sulfate (e.g., Stein et al., 2009; Wang et al., 2011).

3.6. Simulated noise

Random noise was added to laboratory spectra to simulate how spectra of mineral mixtures may appear if observed from orbit. Laboratory spectra were first downsampled to CRISM spectral resolution. A noise scale was defined as a 0–1 influence of random numbers on the vector of a spectrum, implemented using the Matlab `randn` function. One higher noise scale was applied to the wavelength range 1.4–1.5 and 1.9–2.1 μm to account for increased noise in that range due to Mars atmospheric effects (Wiseman et al., 2016; Leask et al., 2018; Itoh and Parente, 2021; Sheppard et al., 2020), and a second lower noise scale applied to the rest of the spectrum. The proper noise scale was calibrated using comparison to actual CRISM spectra of relevant minerals from

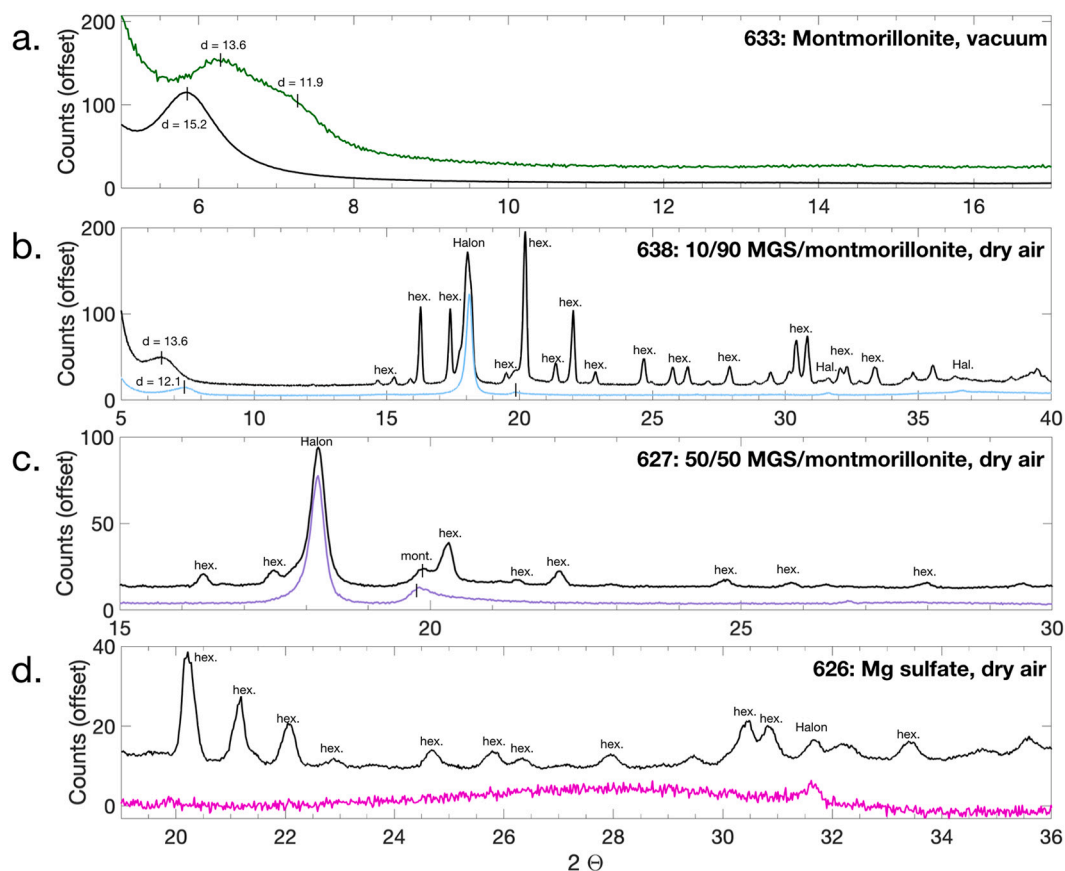


Fig. 3. X-ray diffraction patterns of samples before (black) and after (colors) dehydration. a. Pure montmorillonite dehydrated by exposure to vacuum. b. Physical mixture of 10% Mg sulfate +90% montmorillonite, dehydrated by exposure to dry air. c. Physical mixture of 50% Mg sulfate +50% montmorillonite, dehydrated by exposure to dry air. d. Pure Mg sulfate dehydrated by exposure to dry air.

Gale crater; this process is discussed more in Section 4.5. The final noise scale used were 0.065 and 0.045, respectively, applied over a rolling average window of 3.

4. Results

4.1. X-ray diffraction observations of changes to crystal structure

The effects of dehydration on the crystal structure of montmorillonite, Mg sulfate (MGS), and mixtures thereof can be corroborated using XRD (Fig. 3). In the samples with montmorillonite, the d-spacing of the smectite layers changes from ~ 15 Å at ambient conditions before dehydration to 11–13 Å after dehydration (e.g., Fig. 3a–b.). In samples with any amount of MGS, the MGS XRD peaks at ambient lab conditions were generally most consistent with hexahydrite. In some samples, peaks consistent with epsomite were also present, likely a result of laboratory humidity varying slightly through time (e.g., Supplemental Information Fig. 1). After dehydration, MGS XRD peaks were entirely absent (Fig. 3b–d.).

This lends confidence that changes in the vibrational features observed in the VNIR reflectance spectra, which are sensitive to bonding environments but not necessarily long-range order, can be linked to changes in mineral structure.

4.2. Spectral changes to montmorillonite

Spectral features in the montmorillonite samples that responded most strongly to dehydration were the strength of absorptions associated with H₂O at 1.41, 1.46, 1.91, and 1.96 μm (Fig. 4). The absorptions at 1.41 and 1.91 μm were greatly reduced but not fully removed by the

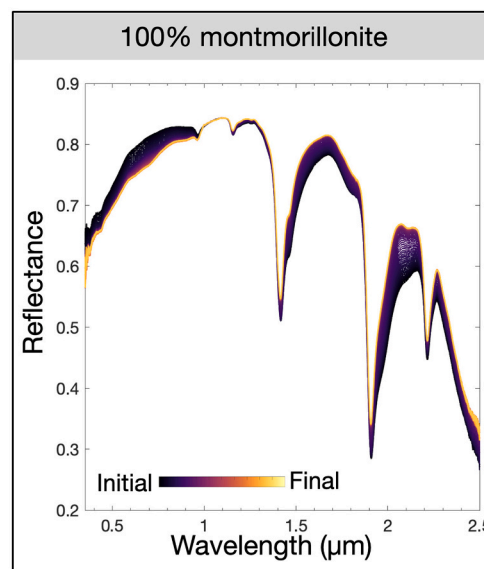


Fig. 4. An example of spectra tracking the dehydration of montmorillonite through time (run 634, dehydration of montmorillonite via increased temperature). Colors represent time, with black spectra from the initial sample and yellow spectra at the end of the run once the montmorillonite was dehydrated. Reflectance is scaled to the maximum value in the initial sample spectrum to more easily compare changes in absorptions; in this case that is at 1.11 μm. (For interpretation of the references to colour in this figure legend, the reader is referred to the web version of this article.)

different methods of dehydration. In contrast, the weaker, adjacent absorptions at 1.46 and 1.96 μm due to H-bonded H_2O in the clay interlayers were fully removed during dehydration. These changes combined affect the overall band shape at both 1.4 and 1.9 μm from a strong asymmetrical V-shaped band with a long-wavelength shoulder in the hydrated samples to a weak almost symmetrical band in the dehydrated samples. These changes can be further examined by plotting the band depth values for both the 1.41 and 1.91 μm absorptions as a function of experimental time (Supplemental Information Figs. 4-5), and both features were observed to decrease at similar rates. Dehydration via low pressure (vacuum) reduces band depth the fastest, followed by dehydration by heating; dehydration by exposure to low %RH dry air is significantly slower. Although rates of change were affected by the dehydration mechanism, the final dehydrated spectra were extremely similar (Supplemental Information Fig. 6).

Weak H_2O overtone absorptions at 0.97 and 1.15 μm also decrease in strength during dehydration, and reflectance values increase at the longest wavelengths in our data that correspond to the short wavelength edge of the broad H_2O fundamental vibration region near $\sim 3 \mu\text{m}$. Although our VNIR data stop at 2.5 μm and do not capture the full evolution of the overlapping vibrations in the 3 μm region, the change in spectral slope that we observe at wavelengths $>2.3 \mu\text{m}$ is consistent with a decrease in the strength of this broad H_2O absorption.

The metal-OH absorption at 2.2 μm also decreases slightly in band depth and band center position during dehydration, despite H_2O nominally not being involved in that bond. This change is presumably an effect of changes in spectral slope that influences the calculated spectral continuum, which in turn can give the appearance of a shift in band position. A true shift in band position should not occur, given that that only H_2O and not OH^- is removed during montmorillonite dehydration (Milliken and Mustard, 2005).

Based on the XRD patterns, the dehydration of montmorillonite leads to the expected reduction (but not full collapse) of the interlayer region (Fig. 3a.). The 001 peak at low 2θ moves to larger 2θ values after dehydration (15.2 to 12–13 \AA), which corresponds to a decrease in the d-

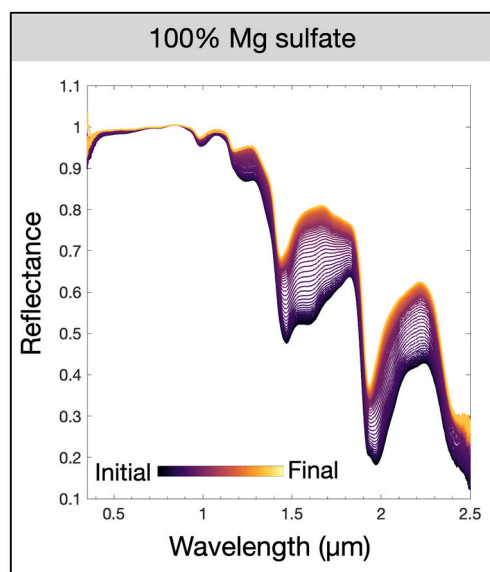


Fig. 5. An example of spectra tracking the dehydration of Mg sulfate through time (run 635, dehydration of Mg sulfate via increased temperature). Colors represent time, with black spectra from the initial sample and yellow spectra at the end of the run once the Mg sulfate was dehydrated and amorphous. Reflectance is scaled to the maximum value in the initial sample spectrum to more easily compare changes in absorptions; in this case that is at 0.837 μm . (For interpretation of the references to colour in this figure legend, the reader is referred to the web version of this article.)

spacing that is consistent with a loss of interlayer H_2O . We note that even after exposure to weak vacuum, some interlayer H_2O remains, as indicated by d-spacing values $>10 \text{\AA}$. This is consistent with the persistence of H_2O absorptions in the spectral data under our experimental conditions.

4.3. Spectral changes to Mg sulfate

Dehydration of MGS affects VNIR spectra much more significantly than in the case of montmorillonite. Band depth values for water-related vibrational absorptions with minima near 0.97, 1.2, 1.5, and 1.95 μm were greatly reduced (Fig. 5). The band center positions of water absorptions also shift to shorter wavelengths. The overall band shape changes significantly, related to mineral restructuring necessary to accommodate changes in hydration state (Wang et al., 2006a, 2006b; Wang et al., 2011; Wang et al., 2016; De Angeles et al., 2017). The 1.5 μm band is extremely broad in hydrated samples and consists of a distinct doublet. Dehydration results in a narrowing of this band to a slightly asymmetric V-shaped absorption with a minimum at 1.45 μm in the final dehydrated spectra. The 1.95 μm absorption exhibits narrow overlapping features at its minimum in the hydrated samples, with a weak but distinct shoulder at 2.05 μm . As in the case of montmorillonite, these longer-wavelength components of the ~ 1.4 and 1.9 μm absorptions disappear quickly and completely during dehydration, whereas the larger absorptions at the shorter wavelength weaken but never fully disappear. In laboratory ambient conditions, the initial MGS was most consistent with hexahydrate/epsomite ($\cdot 6\text{--}7 \text{H}_2\text{O}$), whereas the final dehydrated form of MGS in our experiments is most consistent with $\cdot 2 \text{H}_2\text{O}$ (Chou et al., 2013).

As in dehydration of montmorillonite, vacuum dehydration reduces band depth in MGS spectra the fastest, followed by dehydration by heating; dehydration by exposure to low %RH dry air is slowest (Supplemental Information, Figs. 4–5). Although rates of change were affected by the dehydration mechanism, the final dehydrated spectra were extremely similar (Supplemental Information, Fig. 6). Also similar to dehydration of montmorillonite, the weaker H_2O overtone absorptions at 0.97 and 1.2 μm decrease in strength during dehydration; the 1.2 μm overtone is particularly affected, transitioning from a broad, rounded absorption to a sharper one with a greatly reduced spectral slope in the 1.1–1.3 μm range. As with the montmorillonite, the short wavelength shoulder of the overlapping H_2O vibrations that occur near $\sim 3 \mu\text{m}$ also decrease in strength during dehydration, as indicated by an increase in reflectance values at the longest wavelengths in our data.

Pre-dehydration XRD patterns for the Mg-sulfate (MGS) exhibit peaks consistent with the sulfate being in the form of hexahydrate ($\cdot 6 \text{H}_2\text{O}$), whereas patterns acquired after the dehydration experiments lack peaks and suggest the material has been rendered X-ray amorphous (Fig. 3d.). This transition in hydrous Mg sulfate from a crystalline to amorphous state under Mars-like conditions is consistent with previous studies (Vaniman et al., 2004; Vaniman and Chipera, 2006; Chipera and Vaniman, 2007). Importantly, these XRD patterns confirm that the VNIR spectra acquired under these conditions have captured this phase transition.

4.4. Spectral changes to physical mixtures

Dehydration affects the VNIR spectral absorptions of montmorillonite, Mg sulfate, and physical mixtures of these phases (Fig. 6). The rates of these changes were dependent on the method of dehydration (Supplemental Information, Figs. 4–5). Changes in band depth over the course of the different dehydration experiments are compared in Supplemental Information, Fig. 4. Dehydration under vacuum removes structural water the fastest, followed closely by heating; dehydration by exposure to extremely low RH is the slowest to remove H_2O .

The hydrated 10/90 mixture (10% MGS, 90% montmorillonite) is spectrally similar to pure montmorillonite (Fig. 6a). When fully

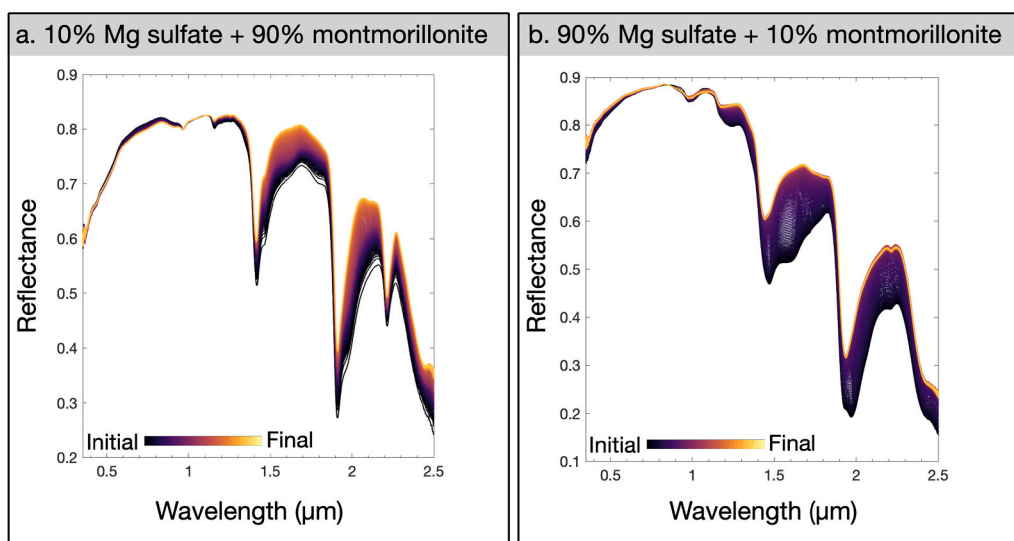


Fig. 6. An example of spectra tracking the dehydration via low RH of physical mixtures of Mg sulfate + montmorillonite through time. Line color represents time, with black spectra from the initial sample and yellow spectra at the end of the run once the mixture was dehydrated. a. Sample 638, dehydration of 10% Mg sulfate + 90% montmorillonite. b. Sample 642, dehydration of 90 wt% Mg sulfate + 10 wt% montmorillonite. Reflectance is scaled to the maximum value in the initial sample spectrum to more easily compare changes in absorptions; in this case that is at (a.) 1.105 μm and (b.) 0.856 μm . (For interpretation of the references to colour in this figure legend, the reader is referred to the web version of this article.)

hydrated, there is some indication of the presence of Mg sulfate ~ 1.95 μm and ~ 1.65 μm . However, within minutes of exposure to low RH, this absorption becomes narrow and spectrally indistinguishable from pure montmorillonite.

The hydrated 90/10 mixture (90% MGS, 10% montmorillonite) is spectrally similar to pure MGS (Fig. 6b). The area most distinct from pure MGS is at 2.2 μm , where the minor presence of montmorillonite still leads to a distinguishable metal-OH absorption in both hydrated and dehydrated samples. The spectrum at wavelengths < 0.8 μm also shows a stronger positive spectral slope than is seen in pure MGS.

The 50/50 mixture is more spectrally similar to montmorillonite than MGS (Supplemental Information Fig. 3f.). The absorptions at 0.97 and 1.15 μm were sharp and only slightly affected by dehydration, closer to what is seen in the pure montmorillonite spectrum. In the 50/50 mixture there is still a perceptible absorption due to MGS at ~ 1.6 – 1.65 μm in the hydrated sample, but this absorption is entirely absent in the dehydrated spectrum.

These similarities between mixtures can be further seen in Fig. 7, which compares the spectra of the dehydrated mixtures, dehydrated pure MGS and montmorillonite, and hydrated MGS and montmorillonite. The dehydrated 90/10 MGS/montmorillonite sample (red) has spectral evidence of both MGS and montmorillonite, but the spectra of the dried 50/50 (orange) and 10/90 (blue) mixtures appear largely indistinguishable from the dried montmorillonite (green), suggesting the montmorillonite masks spectral evidence of MGS when the latter is in a low hydration state. The 1.4 and 1.9 μm bands were somewhat wider than pure montmorillonite, but without foreknowledge of the mineral composition the MGS could go entirely undetected in these spectra. This is in contrast to the spectral modeling results of Stack and Milliken (2013) that indicated low abundances of highly hydrated MGS could be detected when mixed with different smectites, including montmorillonite, and suggests MGS on Mars may be more difficult to detect in NIR spectra when present in the hydrated but amorphous form.

4.5. Adding noise to simulate orbital-quality data

To test our ability to observe the spectral changes in the current generation of orbital VNIR spectral data from Mars, random noise can be added to these laboratory spectra. This allows us to test which features visible in high-quality laboratory data are likely to be obscured if observed from orbit. To calibrate the most appropriate noise levels, we experimented with different intensities of noise until a noised laboratory spectrum of the mineral most closely matched a spectrum of that mineral as observed in Gale crater (unratioed 5×5 averages of CRISM

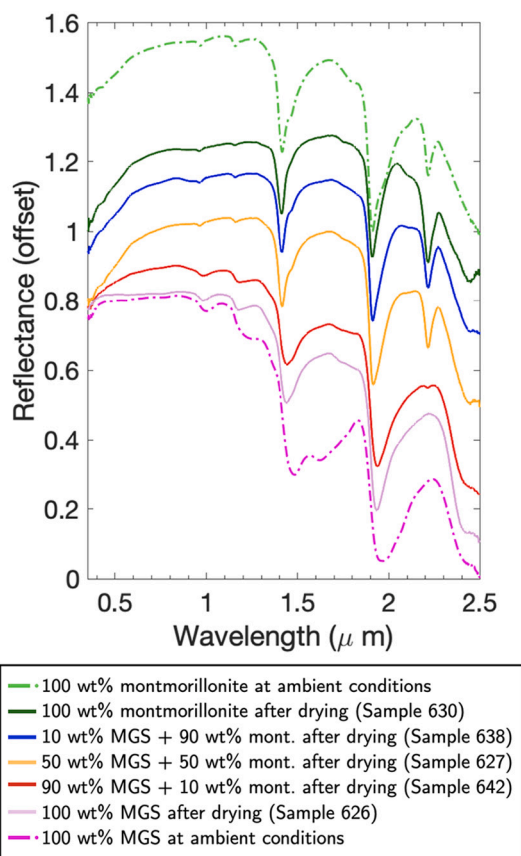


Fig. 7. Spectra of dried minerals and mixtures at the end of dehydration via exposure to dry air (solid lines) and montmorillonite and MGS at ambient (still hydrated) conditions (dashed lines). Reflectance is offset for clarity.

spectra from Sheppard et al., 2020). The results of this step are shown in Fig. 8. The lab spectra were downsampled such that their spectral resolution matched the CRISM data, and randomly generated noise was added to the entire spectrum, with slightly stronger noise in the spectral ranges of 1.4–1.5 and 1.9–2.1 μm where there is a stronger effect of the martian atmosphere (as described in Section 3.6).

To simulate how these subtle spectral changes would manifest in orbital spectra, we then applied this noise addition method (with the

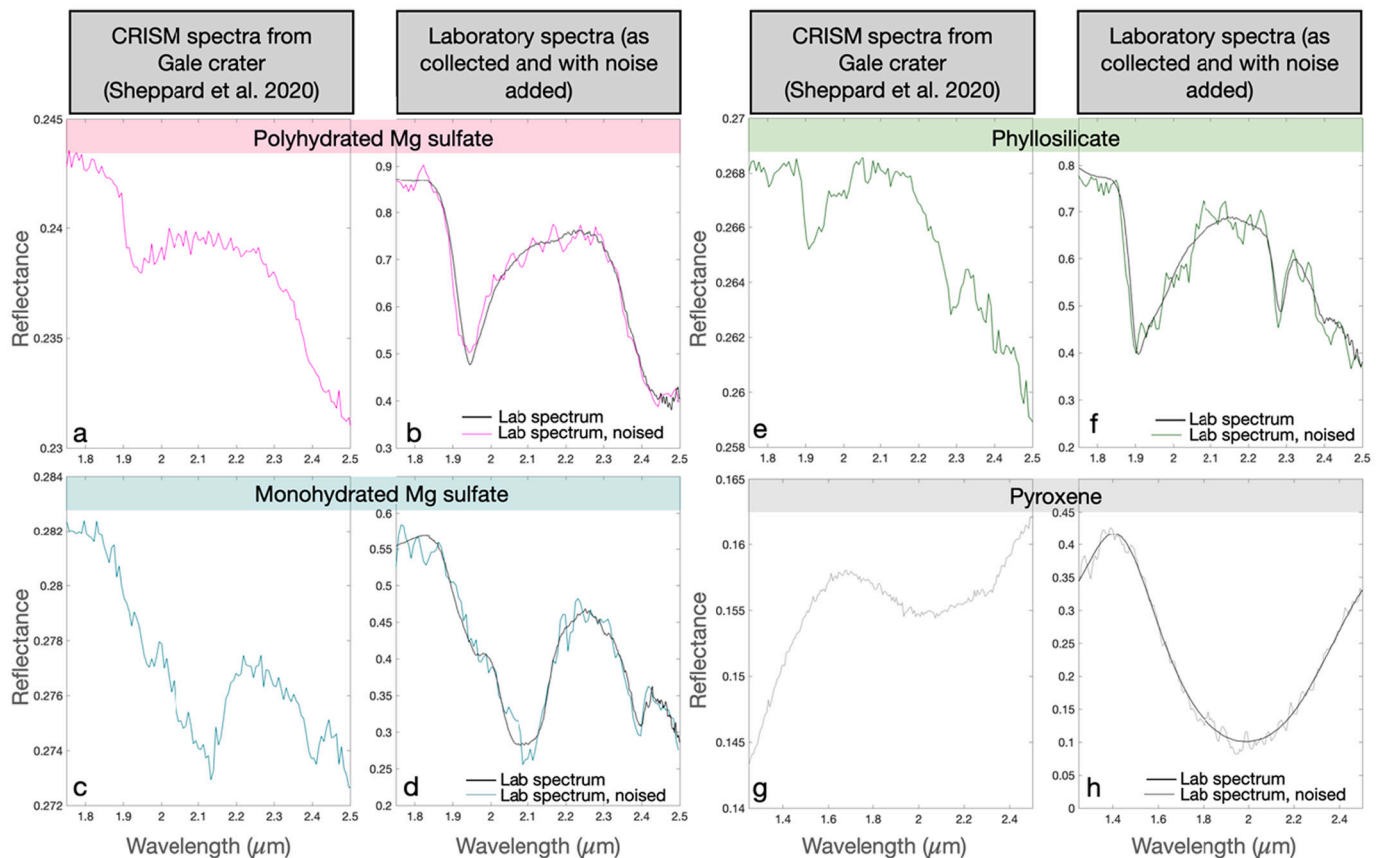


Fig. 8. Noise added to the laboratory data to best match the noise from CRISM data of Gale crater (Sheppard et al., 2020). The left column shows the actual Gale crater CRISM data. The right column shows laboratory spectra of the mineral (black) and the downsampled and noised version of that spectrum that can be considered how that mineral might be observed from orbit via CRISM. The minerals examined are: a-b. polyhydrated Mg sulfate, c-d. monohydrated Mg sulfate, e-f. phyllosilicates, g-h. pyroxene.

same determined noise levels as shown in Fig. 8) to the laboratory spectra from Fig. 7. The results of this are shown in Fig. 9.

5. Discussion

5.1. Mineral structure and hydration state changes in response to Mars-relevant conditions

The change in band minimum position to shorter wavelengths with increasing dehydration is consistent with the loss of loosely held (H-bonded) H₂O (Bishop et al., 1994; Milliken and Mustard, 2005). In montmorillonite, the H₂O absorption with a minimum at ~1.91 μm is associated with a first layer of interlayer H₂O that is bonded to the interlayer cation (primarily Ca in the sample studied here). The longer wavelength shoulder at ~1.95 μm is attributed to successive layers of interlayer H₂O that are H-bonded to the first layer (Bishop et al., 1994). Similar to previous studies, we observe that the ~1.95 μm band disappears first during dehydration, consistent with the loss of the most weakly held H₂O (Bishop et al., 1994; Milliken and Mustard, 2005). All the dehydration experiments presented here resulted in the complete removal of the 1.95 μm absorption, whereas the 1.91 μm band decreased in strength but did not completely disappear. This indicates that even under weak vacuum and very low RH conditions, some H₂O remained in the clay during the duration of the experiments. This is consistent with the observation in XRD patterns that $d(001) > 10 \text{ \AA}$. On these timescales, the water is not fully removed from the montmorillonite structure. It is worth noting that smectites measured *in situ* by CheMin generally do have $d(001) = 10 \text{ \AA}$ (Bristow et al., 2018), perhaps related to their longer period of near-surface exposure or the low RH conditions the sample

cells within the instrument.

As past work has documented (Vaniman et al., 2004; Vaniman and Chipera, 2006; Cloutis et al., 2007; Chou et al., 2013; De Angeles et al., 2017), the MGS system is complicated by irreversible changes to mineral structure. Our results confirm that MGS dehydrates on the timescale of minutes to hours under martian conditions. The final dehydrated form under these conditions is not an anhydrous or even monohydrated kieserite form, but rather a polyhydrated X-ray amorphous form most spectrally consistent with ~2 structural waters (Chou et al., 2013). This amorphous MGS lacks distinct XRD peaks (Fig. 3b-d.). This is consistent with previous dehydration experiments which have shown that XRD peaks associated with crystalline phases can disappear when MGS changes to an amorphous form (Vaniman et al., 2004; Vaniman and Chipera, 2006). The final form of the MGS under dry conditions (similar to some RH conditions experienced on Mars) exhibits no discernible peaks in the XRD patterns.

The effects of dehydration on the spectra of physical mixtures of smectite and MGS are complex. We find that the spectral features of the amorphous MGS are affected when even a small amount of smectite is present but that MGS features are obscured in dehydrated samples with >50% smectite. This is because the width of the 1.9 μm feature associated with MGS is greatly reduced by dehydration, as are the spectral slopes longward of 2.3 μm, thus removing the more diagnostic features of MGS in the mixtures. This suggests that, whereas MGS in the form of epsomite or hexahydrate might be easier to detect when mixed with smectite (e.g., Stack and Milliken, 2013), the unambiguous detection of lower hydration state MGS under lower RH conditions that are more realistic for many locations on Mars may be much more difficult. As MGS dehydrates to the hydrated amorphous form, its spectral features, which

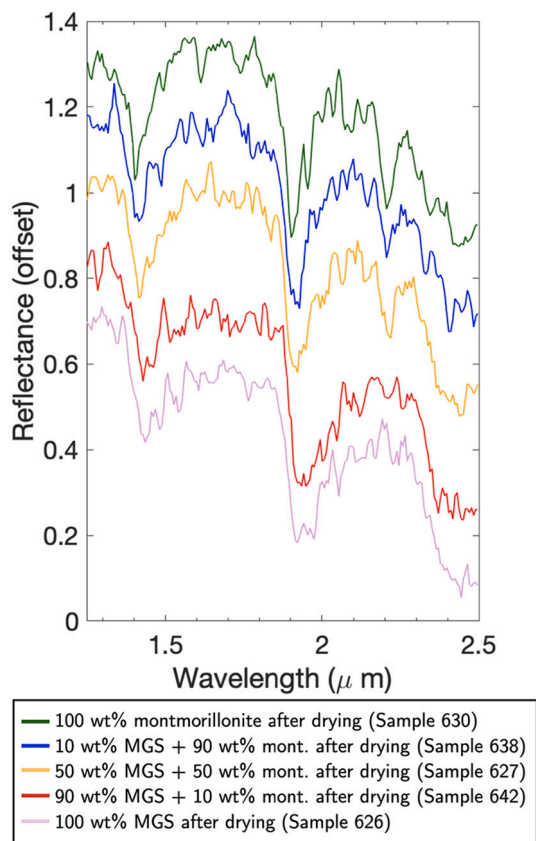


Fig. 9. Downsampled and noised versions of the dehydration experiment spectra from Fig. 7. Noise levels are the same as in Fig. 8, representing how these mineral mixtures might be observed from the martian surface. Reflectance is offset for clarity.

are related primarily to H_2O , become weaker and exhibit more overlap with H_2O features in smectite. If the smectite retains interlayer H_2O then this leads to spectral masking of the MGS. The opposite is not necessarily true because smectites exhibit diagnostic OH-related absorptions in the ~ 2.2 – $2.5 \mu m$ range that are unaffected by RH and can be discerned if at least $\sim 10\%$ smectite is present. These results underscore the significance that H_2O -related absorptions can have in the identification and detection of hydrous minerals and the importance of measuring such minerals under relevant RH conditions to properly understand detection limits on Mars using NIR reflectance spectroscopy.

In addition to the above mentioned spectral masking effects, nonlinear spectral mixing effects can also result in cases where two distinct mixtures exhibit similar or indistinguishable spectra. Multiple scattering effects and nonlinear absorption processes are inherent to VNIR spectral analysis of intimate mineral mixtures, meaning reflectance spectra of complex mineral assemblages typically cannot be modeled as a simple linear combination of individual component spectra weighted by their fractional volumes (Clark, 1983; Hapke, 1993; Poulet and Erard, 2004). Several characteristics contribute to nonlinearity in the relative contributions of mixture components to the final spectrum, including the confounding effects of strongly varying absorption coefficients, surface textures, porosity, and particle size (Clark and Roush, 1984; Mustard and Pieters, 1987; Hapke, 1993; Poulet and Erard, 2004; Farrand et al., 2006; Milliken and Mustard, 2007a,b). In this contribution we highlight a situation where assessment of orbital and laboratory spectra have the potential to lead to consistent non-detection of phases, in this case MGS in a low hydration state.

5.2. Implications for orbital observation

Our laboratory results suggest that hydrated and partially dehydrated clays and sulfates are spectrally distinct, but that the presence of smectites can mask the presence of low hydration state Mg-sulfate. Indeed, it is difficult to unambiguously detect even 50% MGS when mixed with smectite (Fig. 7) under the low RH conditions explored here, especially when noise is added to the high SNR lab spectra. These results predict that polyhydrated MGS on the martian surface, which in many locations is likely to be X-ray amorphous and bearing 2 structural waters, may be much more widespread in clay-bearing regions than currently recognized based on orbital VNIR spectra.

Based on the results presented here and the similarity in spectral modeling results of MGS mixed with various smectites published by Stack and Milliken (2013), we propose that these experiments on montmorillonite are applicable to a broader range of martian smectites. The type of smectite formed during alteration processes is driven by the parent material, the fluid salinity and pH, and the degree of alteration (Weaver, 1989; Chamley, 1989; Meunier, 2005; Tu et al., 2021), and nontronite, montmorillonite, and saponite can all form in slightly acidic to neutral pH fluids (Harder, 1972; Harder, 1976; Decarreau and Bonnin, 1986; Decarreau et al., 1987; Vogels et al., 1995; Tu et al., 2021). Aluminous smectites such as montmorillonite (metal-OH absorption $\sim 2.21 \mu m$) are present on Mars, as are Fe/Mg smectites such as nontronite (metal-OH absorption $\sim 2.28 \mu m$) and saponite (metal-OH absorption $\sim 2.3 \mu m$) (Poulet et al., 2005; Mustard et al., 2008; Ehlmann et al., 2011; Carter et al., 2013; Sheppard et al., 2021; Tu et al., 2021). Because of spectral effects due to atmospheric absorptions and Fe-rich dust, discerning between smectites on Mars using CRISM and OMEGA data relies primarily on the position of the metal-OH absorption. Furthermore, many clay deposits on Mars may be of mixed clay mineralogy, with spectra not perfectly matching one mineral endmember (Milliken and Bish, 2010; Sheppard et al., 2021; Tu et al., 2021). Additional laboratory experiments investigating the interplay of sulfate and smectite spectral features using additional smectites would be of value and we propose the effects we observe in the case of montmorillonite are likely to apply to other smectites, particularly because the primary effects are associated with changes in the H_2O features that are known to be similar between different smectites. Because purely binary physical mixtures of smectite and sulfate are unlikely to exist on Mars, studies of spectral changes on a more mineralogically diverse regolith simulant with anhydrous as well as hydrous phases would also be valuable.

Many of the spectral changes observed during the process of dehydration may be too subtle to be observed in visual inspection of orbital spectral data (Fig. 9), and the same would be true for hydration reactions that induce similar small spectral changes. The $1.4 \mu m$ absorption is a relatively small and subtle feature, while the longer wavelength portion of the $1.9 \mu m$ absorption can be affected by atmospheric absorptions. The $1.95 \mu m$ shoulder exhibits some of the strongest spectral changes (e.g., Fig. 6), but these changes may be confounded by the presence of atmospheric CO_2 absorptions in actual NIR spectra of Mars. Therefore, it may be most conclusive to use the $1.91 \mu m$ feature to look for hydration changes in VNIR spectra of hydrous mineral deposits on Mars. Confirming these hydration state changes would require repeat observations, including during times of high RH (low temperature).

Based on the results that (1) polyhydrated MGS is likely in an amorphous form at martian surface conditions, and (2) spectral evidence of amorphous MGS can be obscured by hydrated phyllosilicates (and even more so with decreasing signal-to-noise levels), it is possible that MGS is currently under-detected on the martian surface and may be present in some clay-bearing terrains but not visible from orbit. While the presence of amorphous MGS may impart a somewhat wider $1.9 \mu m$ band (Fig. 9), at CRISM resolution its presence is likely to be quite subtle, especially if clay minerals are present in the same pixel.

This possibility would require additional *in situ* exploration to test. It

is consistent with what has been observed from orbit at Gale crater, where observation of VNIR spectra has shown clays and sulfates occur in a range of stratigraphic positions, with lower strata more enriched in phyllosilicates and upper strata more enriched in sulfates (Milliken et al., 2010; Fraeman et al., 2016; Sheppard et al., 2020). A zone of kieserite-rich bedrock of variable thickness is stratigraphically restricted but traceable around Mt. Sharp. It appears, therefore, to be a confined but throughgoing zone embedded within a thick sequence of polyhydrated MGS-rich strata. In one area with low topographic slopes, kieserite and polyhydrated MGS appear to be intercalated (possibly interbedded) in meters-scale zones that are distinct from each other in albedo and spectral signature.

Given the Curiosity rover evolved gas analysis (EGA) observations of Mg sulfate within the sediments of Mt. Sharp (Sutter et al., 2017), the current lack of observed crystalline Mg sulfate in CheMin XRD data, and our experimental results showing MGS is stable in X-ray amorphous polyhydrated form under a range of martian conditions, we conclude that a significant portion of Mg sulfate inferred from VNIR orbital spectra of Gale crater (Milliken et al., 2010; Fraeman et al., 2016; Sheppard et al., 2020) is likely in a hydrated X-ray amorphous form. X-ray amorphous material has been measured in every drill hole within Mt. Sharp (Rampe et al., 2017; Smith et al., 2018; Achilles et al., 2020; Smith et al., 2021), increasing the likelihood of these phases being active in the modern hydrological cycle. This is further illustrated in Fig. 7: pure dehydrated MGS has observable MGS spectral features; however, in the dehydrated samples with >10 wt% montmorillonite, the montmorillonite spectral features overwhelm the spectral features of amorphous MGS. Samples analyzed by CheMin sit in a relatively warm and dry chamber for several hours before and during analysis, which is enough to dehydrate gypsum to bassanite (Vaniman et al., 2018). This environment is also possibly dry enough to render any MGS in a drilled sample amorphous even if it is actually crystalline in the rock prior to drilling.

However, given the other lines of evidence, the crystalline MGS may have precipitated during primary or diagenetic aqueous processes and surface exposure allowed for dehydration to an amorphous polyhydrated form. This would be consistent with both the orbital identification of hydrous Mg sulfate in Mt. Sharp and the lack of a clear crystalline Mg sulfate phase in the rover XRD data.

In addition, although the results present here do not provide a definitive solution to the “missing salts” conundrum posed by Milliken et al. (2009), they do highlight that spectral masking of salts, and MGS in particular, should not be readily discounted. Further study of mixtures of hydrous minerals under Mars-like conditions is clearly warranted to better understand the range of phases that may have so far gone undetected (and are perhaps undetectable) in VNIR data even when present in high abundances. Resolving this question for individual regions on Mars may require *in situ* observations specifically designed with the capability to identify and characterize poorly crystalline amorphous phases.

Understanding the possible extent of hydrous salts on Mars is critical, as previous work has shown that some amorphous salts readily exchange water with the martian atmosphere and may thus be active participants in the modern hydrological cycle (e.g., Sklute et al., 2018). It has been theorized that the extra availability of exchangeable water in smectite-sulfate mixtures may obscure the link between atmospheric conditions and preserved hydration state, with sulfate hydration state depending more on local water exchange within the rock/regolith than on atmospheric %RH (Wilson and Bish, 2012). Given these constraints, different formation mechanisms or exposure histories may be required to explain the orbital detections of both kieserite and polyhydrated MGS at the martian surface, including in Gale crater. Past work has suggested that the skin depth for hydrous mineral exchange is likely to be millimeters to centimeters on a daily scale and 10s of centimeters on a seasonal scale (Schorghofer and Aharonson, 2005; Vaniman and Chipera, 2006). This is significant enough to affect the optical surface, even on a diurnal

timescale. Further laboratory experiments and *in situ* observations to estimate this skin depth will move us toward being able to estimate the true size of this water reservoir on Mars.

6. Conclusions

Dehydration experiments of Ca-rich montmorillonite and polyhydrated Mg sulfate under dry conditions relevant to Mars confirm that both minerals have the potential to be active in the martian hydrological cycle and that Mg sulfate is likely under-detected from orbit. We find that dehydration occurs relatively rapidly in all samples and causes distinct changes to VNIR spectra and X-ray diffraction data. Dehydration to Mars-relevant conditions reduces montmorillonite to 1 water layer and Mg sulfate to an X-ray amorphous polyhydrated form with 2 structural waters. Dehydration of mixtures of $\geq 50\%$ montmorillonite and $\leq 50\%$ Mg sulfate are spectrally indistinguishable from dehydrated pure montmorillonite. Because smectite is both widespread across the martian surface and efficient at masking spectral features of low hydration state, amorphous Mg sulfate, we conclude that Mg sulfate is likely under-identified from orbit, including in Gale crater, and may be more common in ancient Noachian clay-bearing terrains than previously recognized.

Declaration of Competing Interest

None.

Acknowledgments

We would like to acknowledge funding from the NASA MSL Participating Scientist Program. We also acknowledge the MRO CRISM, HiRISE, MSL, and CTX science teams. The research was carried out at the Jet Propulsion Laboratory, California Institute of Technology, under a contract with the National Aeronautics and Space Administration (80NM0018D0004).

Appendix A. Supplementary data

Supplementary data to this article can be found online at <https://doi.org/10.1016/j.icarus.2022.115083>.

References

- Achilles, C.N., Rampe, E.B., Downs, R.T., Bristow, T.F., Ming, D.W., Morris, R.V., Vaniman, D.T., Blake, D.F., Yen, A.S., McAdam, A.C., Sutter, B., Fedo, C.M., Gwizd, S., Thompson, L.M., Gellert, R., Morrison, S.M., Treiman, A.H., Crisp, J.A., Gabriel, T.S.J., Chipera, S.J., Hazen, R.M., Craig, P.I., Thorpe, M.T., Des Marais, D.J., Grotzinger, J.P., Tu, V.M., Castle, N., Downs, G.W., Peretyazhko, T.S., Walroth, R.C., Sarrazin, P., Morookian, J.M., 2020. Evidence for Multiple Diagenetic Episodes in Ancient Fluvial-Lacustrine Sedimentary Rocks in Gale Crater, Mars. *J. Geophys. Res.: Planets* 125, e2019JE006295. <https://doi.org/10.1029/2019JE006295>.
- Beck, P., Pommerol, A., Schmitt, B., Brissaud, O., 2010. Kinetics of water adsorption on minerals and the breathing of the Martian regolith. *J. Geophys. Res.* 115, E10011.
- Bibring, Jean-Pierre, Langevin, Yves, Gendrin, Aline, Gondet, Brigitte, Poulet, Francois, Berthé, Michel, Soufflot, Alain, Arvidson, Ray, Mangold, Nicolas, Mustard, John, Drossart, P., and the OMEGA team, 2005. Mars Surface Diversity as Revealed by the OMEGA/Mars Express Observations. *Science* 307, 1576–1581.
- Bibring, Jean-Pierre, Langevin, Yves, Mustard, John F., Poulet, Francois, Arvidson, Raymond, Gendrin, Aline, Gondet, Brigitte, Mangold, Nicolas, Pinet, P., Forget, F., the OMEGA team, 2006. Global mineralogical and aqueous Mars history derived from OMEGA/Mars express data. *Science* 312, 400–404.
- Bish, David L., William Carey, J., Vaniman, David T., Chipera, Steve J., 2003. Stability of hydrous minerals on the martian surface. *Icarus* 164, 96–103.
- Bishop, Janice L., Pieters, Carle M., 1995. Low-temperature and low atmospheric pressure infrared reflectance spectroscopy of Mars soil analog materials. *J. Geophys. Res.* 100 (E3), 5369–5379.
- Bishop, Janice L., Pieters, Carle M., Edwards, John O., 1994. Infrared spectroscopic analyses on the nature of water in montmorillonite. *Clay Clay Miner.* 42 (6), 702–716.
- Bishop, J.L., Lane, M.D., Dyar, M.D., Brown, A.J., 2008. Reflectance and emission spectroscopy study of four groups of phyllosilicates: smectites, kaolinite-serpentines, chlorites and micas. *Clay Miner.* 43 (1), 35–54.

- Bishop, Janice L., Parente, Mario, Weitz, Catherine M., Noe Dobrea, Eldar Z., Roach, Leah H., Murchie, Scott L., McGuire, Patrick C., McKeown, Nancy K., Rossi, Christopher M., Brown, Adrian J., Calvin, Wendy M., Milliken, Ralph, Mustard, John F., 2009. Mineralogy of Juventae Chasma: Sulfates in the light-toned mounds, mafic minerals in the bedrock, and hydrated silica and hydroxylated ferric sulfate on the plateau. *J. Geophys. Res.* 114.
- Bristow, Thomas F., Rampe, Elizabeth B., Achilles, Cherie N., Blake, David F., Chipera, Steve J., Craig, Patricia, Crisp, Joy A., Des Marais, David J., Downs, Robert T., Gellert, Ralf, Grotzinger, John P., Gupta, Sanjeev, Hazen, Robert M., Horgan, Briony, Hogancamp, Joanna V., Mangold, Nicolas, Mahaffy, Paul R., McAdam, Amy C., Ming, Doug W., Morokian, John Michael, Morris, Richard V., Morrison, Shaunna M., Treiman, Allan H., Vaniman, David T., Vasavada, Ashwin R., Yen, Albert S., 2018. Clay mineral diversity and abundance in sedimentary rocks of Gale crater, Mars. *Mars. Sci. Adv.* 4.
- Carter, J., Poulet, F., Bibring, J.-P., Mangold, N., Murchie, S., 2013. Hydrous minerals on Mars as seen by the CRISM and OMEGA imaging spectrometers: Updated global view. *J. Geophys. Res.* 118, 1–28.
- Chamley, H., 1989. *Clay Mineralogy*. Springer, Berlin, Germany, p. 623.
- Chipera, Steve J., Vaniman, David T., 2007. Experimental stability of magnesium sulfate hydrates that may be present on Mars. *Geochim. Cosmochim. Acta* 71, 241–250.
- Chou, I.-M., Seal II, R.R., 2003. Determination of epsomite-hexahydrate equilibria by the humidity-buffer technique at 0.1 MPa with implications for phase equilibria in the system MgSO₄-H₂O. *Astrobiology* 3, 619–630.
- Chou, I-Ming, Seal, Robert R., Wang, Alian, 2013. The stability of sulfate and hydrated sulfate minerals near ambient conditions and their significance in environmental and planetary sciences. *J. Asian Earth Sci.* 62, 734–758.
- Clark, Roger N., 1981. The spectral reflectance of water-mineral mixtures at low temperatures. *J. Geophys. Res.* 86 (B4), 3074–3086.
- Clark, R.N., Roush, T.L., 1984. Reflectance spectroscopy: quantitative analysis techniques for remote sensing applications. *JGR* 89 (7), 6329–6340.
- Clark, R.N., 1983. Spectral properties of mixtures of montmorillonite and dark carbon grains: Implications for remote sensing minerals containing chemically and physically adsorbed water. *J. Geophys. Res.* 88, 635–644, 10.
- Clark, R.N., King, T.V.V., Klejwa, M., Swayze, G.A., Vergo, N., 1990. High spectral resolution reflectance spectroscopy of minerals. *J. Geophys. Res. Solid Earth* 95 (B8), 12653–12680.
- Cloutis, Edward A., Hawthorne, Frank C., Mertzman, Stanley A., Krenn, Katherine, Craig, Michael A., Marcino, Dionne, Methot, Michelle, Strong, Johnathon, Mustard, John F., Blaney, Diana L., Bell, James F., Vilas, Faith, 2006. Detection and discrimination of sulfate minerals using reflectance spectroscopy. *Icarus* 184 (1), 121–157.
- Cloutis, E.A., Craig, M.A., Mustard, J.F., Kruzelecky, R.V., Jamroz, W.R., Scott, A., Bish, D.L., Poulet, F., Bibring, J.-P., King, P.L., 2007. Stability of hydrated minerals on Mars. *Geophys. Res. Lett.* 34, L20202.
- Cloutis, E.A., Craig, M.A., Kruzelecky, R.V., Jamroz, W.R., Scott, A., Hawthorne, F.C., Mertzman, S.A., 2008. Spectral reflectance properties of minerals exposed to simulated Mars surface conditions. *Icarus* 195, 140–168.
- De Angeles, S., Carli, C., Tosi, F., Beck, P., Piccioni, G., De Sanctis, M.C., Capaccioni, F., Di Iorio, T., Philippe, S., 2017. Temperature-dependent VNIR spectroscopy of hydrated Mg-sulfates. *Icarus* 281, 444–458.
- Decarreau, A., Bonnin, D., 1986. Synthesis and crystallogensis at low temperature of Fe (III)-smectites by evolution of coprecipitated gels: Experiments in partially reducing conditions. *Clay Miner.* 21, 861–877.
- Decarreau, A., Bonnin, D., Badaut-Trauth, D., Couty, R., Kaiser, P., 1987. Synthesis and crystallogensis of ferric smectite by evolution of Si-Fe coprecipitates in oxidizing conditions. *Clay Miner.* 22, 207–223.
- Ehlmann, B.L., Mustard, J.F., Fassett, C.I., Schon, S.C., Head III, J.W., Des Marais, D.J., Grant, J.A., Murchie, S.L., 2008. Clay minerals in delta deposits and organic preservation potential on Mars. *Nat. Geosci.* 1, 355–358.
- Ehlmann, Bethany, Berger, Gilles, Mangold, Nicolas, Michalski, Joseph, Catling, David, Ruff, Steven, Chassefière, Eric, Niles, Paul, Chevrier, Vincent, Poulet, Francois, 2013. Geochemical Consequences of Widespread Clay Mineral Formation in Mars' Ancient Crust. *Space Sci. Res.* 174, 329–364. <https://doi.org/10.1007/s11214-012-9930-0>.
- Ehlmann, B.L., Mustard, J.F., Murchie, S.L., Bibring, J.-P., Meunier, A., Fraeman, A.A., Langevin, Y., 2011. Subsurface water and clay mineral formation during the early history of Mars. *Nature* 479, 53–60.
- Farrand, W.H., Bell III, J.F., Johnson, J.R., Squyres, S.W., Soderblom, J., Ming, D.W., 2006. Spectral variability among rocks in visible and near-infrared multispectral Pancam data collected at Gusev crater: Examinations using spectral mixture analysis and related techniques. *JGR*, 111, p. E02S15.
- Fialips, Claire, Carey, J. William, Vaniman, David T., Bish, David L., Feldman, William C., Mellon, Michael T., 2005. Hydration state of zeolites, clays, and hydrated salts under present-day martian surface conditions: Can hydrous minerals account for Mars Odyssey observations of near-equatorial water-equivalent hydrogen? *Icarus* 178, 74–83.
- Fraeman, A., Ehlmann, B.L., Arvidson, R.E., Edwards, C.S., Grotzinger, J.P., Milliken, R. E., Quinn, D.P., Rice, M.S., 2016. The stratigraphy and evolution of lower Mount Sharp from spectral, morphological, and thermophysical orbital data sets. *J. Geophys. Res. Planets* 121, 1713–1736.
- Gendrin, Aline, Mangold, Nicolas, Bibring, Jean-Pierre, Langevin, Yves, Gondet, Brigitte, Poulet, Francois, Bonello, Guillaume, Quantin, Cathy, Mustard, John, Arvidson, Ray, LeMouelic, Stephane, 2005. Sulfates in martian layered terrains: the OMEGA/Mars express view. *Science* 307, 1587–1591.
- Grotzinger, J.P., Sumner, D.Y., Kah, L.C., Stack, K., Gupta, S., Edgar, L., Rubin, D., Lewis, K., Schieber, J., Mangold, N., Milliken, R., Conrad, P.G., DesMarais, D., Farmer, J., Siebach, K., Calef III, F., Hurowitz, J., McLennan, S.M., Ming, D., Vaniman, D., Crisp, J., Vasavada, A., Edgett, K.S., Malin, M., Blake, D., Gellert, R., Mahaffy, P., Wiens, R.C., Maurice, S., Grant, J.A., Wilson, S., Anderson, R.C., Beegle, L., Arvidson, R., Hallet, B., Sletten, R.S., Rice, M., Bell III, J., Griffes, J., Ehlmann, B., Anderson, R.B., Bristow, T.F., Dietrich, W.E., Dromart, G., Eigenbrode, J., Fraeman, A., Hardgrove, C., Herkenhoff, K., Jandura, L., Kocurek, G., Lee, S., Leshin, L.A., Leveille, R., Limonadi, D., Maki, J., McCloskey, S., Meyer, M., Minitti, M., Newsom, H., Oehler, D., Okon, A., Palucis, M., Parker, T., Rowland, S., Schmidt, M., Squyres, S., Steele, A., Stolper, E., Summons, R., Treiman, A., Williams, R., Yingst, A., 2014. A habitable fluvio-lacustrine environment at Yellowknife Bay, Gale Crater, Mars. *Science* 343.
- Hapke, B.W., 1993. *Theory of Reflectance and Emittance Spectroscopy*. Cambridge Univ. Press, Cambridge, UK, p. 455.
- Harder, H., 1972. The role of magnesium in the formation of smectite minerals. *Chem. Geol.* 10, 31–39.
- Harder, H., 1976. Nontronite synthesis at low temperatures. *Chem. Geol.* 18, 169–180.
- Hess, S.L., Ryan, J.A., Tillman, J.E., Henry, R.M., Leov, C.B., 1979. The annual cycle of pressure on Mars measured by Viking landers 1 and 2. *Geophys. Res. Lett.* 7 (3), 197–200.
- Hogenboom, D.L., Kargel, J.S., Ganasan, J.P., Lee, L., 1995. Magnesium sulfate-water to 400 MPa using a novel piezometer: densities, phase equilibria, and planetological implications. *Icarus* 115, 258–277.
- Itoh, Yuki, Parente, Mario, 2021. A new method for atmospheric correction and denoising of CRISM hyperspectral data. *Icarus* 354 (114024).
- Jakosky, Bruce M., Jones, John H., 1997. The history of martian volatiles. *Rev. Geophys.* 35 (1), 1–16.
- Jamieson, S., Noe Dobrea, E.Z., Dalton, J.B., Pitman, K.M., Abbey, W.J., 2014. The spectral variability of kieserite (MgSO₄-H₂O) with temperature and grain size and its application to the martian surface. *J. Geophys. Res. Planets* 119, 1218–1237.
- Leask, E.K., Ehlmann, B.L., Dundar, M.M., Murchie, S.L., Seelos, F.P., 2018. Challenges in the search for perchlorate and other hydrated minerals with 2.1- μ m absorptions on Mars. *Geophys. Res. Lett.* 45, 12180–12189.
- Mangold, Nicolas, Gendrin, Aline, Gondet, Brigitte, LeMouelic, Stephane, Quantin, Cathy, Ansan, Veronique, Bibring, Jean-Pierre, Langevin, Yves, Masson, Philippe, Neukum, Gerhard, 2008. Spectral and geological study of the sulfate-rich region of West Candor Chasma, Mars. *Icarus* 113, E08009. <https://doi.org/10.1029/2007JE002985>.
- Martin-Torres, F. Javier, Zorzano, Maria-Paz, Valentin-Serrano, Patricia, Harri, Ari-Matti, Genzer, Maria, Kempainen, Osku, Rivera-Valentin, Edgar G., Jun, Insoo, Wray, James, Madsen, Morten Bo, Goetz, Walter, McEwen, Alfred S., Hardgrove, Craig, Renno, Nilton, Chevrier, Vincent F., Mischna, Michael, Navarro-Gonzalez, Rafael, Martinez-Frias, Jesus, Conrad, Pamela, McConnochie, Tim, Cockell, Charles, Berger, Gilles, Vasavada, Ashwin R., Sumner, Dawn, Vaniman, David, 2015. Transient liquid water and water activity at Gale crater on Mars. *Nat. Geosci.* 8 <https://doi.org/10.1038/NNGEO2412>.
- McKeown, Nancy, Bishop, Janice, Noe Dobrea, Eldar, Ehlmann, Bethany, Parente, Mario, Mustard, John, Murchie, Scott, Swayze, Greg, Bibring, Jean-Pierre, Silver, Eli, 2009. Characterization of phyllosilicates observed in the central Mawrth Vallis region, Mars, their potential formational processes, and implications for past climate. *J. Geophys. Res.* 114 (E00D10) <https://doi.org/10.1029/2008JE003301>.
- McLennan, Scott M., Grotzinger, John P., Hurowitz, Joel A., Tosca, Nicholas J., 2018. The sedimentary cycle on early Mars. *Annu. Rev. Earth Planet. Sci.* 47, 91–118.
- Meunier, A., 2005. *Clays*. Springer, Berlin, Germany, p. 472.
- Milliken, R.E., Bish, D.L., 2010. Sources and sinks of clay minerals on Mars. In: *Philosophical Magazine*, Vol. 90, pp. 2293–2308. Nos. 17–18, 14–28.
- Milliken, R.E., Mustard, J.F., 2005. Quantifying Absolute Water Content of Minerals using Near-Infrared Reflectance Spectroscopy. *JGR*, 110, p. E12001. <https://doi.org/10.1029/2005JE002534>.
- Milliken, R.E., Fischer, W.W., Hurowitz, J.A., 2009. Missing Salts on EARLY MARS, GRL, 36, p. L11202.
- Milliken, R.E., Grotzinger, J.P., Thompson, B.J., 2010. Paleoclimate of Mars as captured by the stratigraphic record in Gale Crater. *Geophys. Res. Lett.* 37 <https://doi.org/10.1029/2009GL041870>.
- Milliken, Ralph, Mustard, John, 2007. Estimating the water content of hydrated minerals using reflectance spectroscopy I. Effects of darkening agents and low-albedo materials. *Icarus* 189, 550–573.
- Milliken, Ralph, Mustard, John, 2007. Estimating the water content of hydrated minerals using reflectance spectroscopy II. Effects of particle size. *Icarus* 189, 574–588.
- Murchie, Scott, Roach, Leah, Seelos, Frank, Milliken, Ralph, Mustard, John, Arvidson, Raymond, Wiseman, Sandra, Lichtenberg, Kimberly, Andrews-Hanna, Jeffrey, Bishop, Janice, Bibring, Jean-Pierre, Parente, Mario, Morris, Richard, 2009. Evidence for the origin of layered deposits in Candor Chasma, Mars, from mineral composition and hydrologic modeling. *J. Geophys. Res.* 114, E00D05 <https://doi.org/10.1029/2009JE003343>.
- Mustard, J.F., Murchie, S.L., Pelkey, S.M., Ehlmann, B.L., Milliken, R.E., Grant, J.A., Bibring, J.-P., Poulet, F., Bishop, J., Dobrea, E.N., Roach, L., Seelos, F., Arvidson, R. E., Wiseman, S., Green, R., Hash, C., Humm, D., Malaret, E., McGovern, J.A., Seelos, K., Clancy, T., Clark, R., Des Marais, D., Izenberg, N., Knudson, A., Langevin, Y., Martin, T., McGuire, P., Morris, R., Robinson, M., Roush, T., Smith, M., Swayze, G., Taylor, H., Titus, T., Wolff, M., 2008. Hydrated silicate minerals on Mars observed by the Mars Reconnaissance Orbiter CRISM instrument. *Nature* 454, 305–309.
- Mustard, J.F., Pieters, C.M., 1987. Quantitative Abundance Estimates From Bidirectional Reflectance Measurements. *J. Geophys. Res.* 92, E617–E626. B4.
- Noe Dobrea, E.Z., Bishop, J.L., McKeown, N.K., Fu, R., Rossi, C.M., Michalski, J.R., Heinlein, C., Hanus, V., Poulet, F., Mustard, J.F., Murchie, S., McEwen, A.S., Swayze, G., Bibring, J.-P., Malaret, E., Hash, C., 2010. Mineralogy and stratigraphy

- of phyllosilicate-bearing and dark mantling units in the greater Mawrth Vallis/west Arabia Terra area: Constraints on geological origin. *Journal of Geophysical Research* 115. <https://doi.org/10.1029/2009JE003351>.
- Pitman, Karly M., Noe Dobra, Eldar Z., Jamieson, Corey S., Dalton, James B., Abbey, William J., Joseph, Emily C.S., 2014. Reflectance spectroscopy and optical functions for hydrated Fe-sulfates. *Am. Mineral.* 99 (8–9), 1593–1603. <https://doi.org/10.2138/am.2014.4730>.
- Pommerol, Antoine, Schmitt, Bernard, Beck, Pierre, Brissaud, Olivier, 2009. Water sorption on martian regolith analogs: Thermodynamics and near-infrared reflectance spectroscopy. *Icarus* 204, 114–136.
- Poulet, F., Erard, S., 2004. Nonlinear spectral mixing: Quantitative analysis of laboratory mineral mixtures. *J. Geophys. Res.* 109, E02009. <https://doi.org/10.1029/2003JE002179>.
- Poulet, F., Bibring, J.P., Mustard, J.F., Gendrin, A., Mangold, N., Langevin, Y., Arvidson, R.E., Gondet, Gomez, Berthe, M., Erard, S., Forni, O., Manaud, N., Poulleau, G., Soufflot, A., Combes, M., Drossart, P., Encrenaz, T., Fouchet, T., Melchiorri, R., Bellucci, G., Altieri, F., Formisano, V., Fonti, S., Capaccioni, F., Ceroni, P., Coradini, A., Korablev, O., Kottsov, V., Ignatiev, N., Titov, D., Zasova, L., Pinet, P., Schmitt, B., Sotin, C., Hauber, E., Hoffmann, H., Jaumann, R., Keller, U., Forget, F., 2005. and the Omega Team. Phyllosilicates on Mars and implications for early martian climate. *Nature* 438, 623–627.
- Rampe, E.B., Ming, D.W., Blake, D.F., Bristow, T.F., Chipera, S.J., Grotzinger, J.P., Morris, R.V., Morrison, S.M., Vaniman, D.T., Yen, A.S., Achilles, C.N., Craig, P.I., Marais, D.J. Des, Downs, R.T., Farmer, J.D., Fendrich, K.V., Gellert, R., Hazen, R.M., Kah, L.C., Morookian, J.M., Peretyazhko, T.S., Sarrazin, P., Treiman, A.H., Berger, J. A., Eigenbrode, J., Fairen, A.G., Forni, O., Gupta, S., Hurowitz, J.A., Lanza, N.L., Schmidt, M.E., Siebach, K., Sutter, B., Thompson, L.M., 2017. Mineralogy of an ancient lacustrine mudstone succession from the Murray formation, Gale crater, Mars. *EPSL* 471, 172–185.
- Rapin, W., Ehlmann, B.L., Dromart, G., Schieber, J., Thomas, N.H., Fischer, W.W., Fox, V. K., Stein, N.T., Nachon, M., Clark, B.C., Kah, L.C., Thompson, L., Meyer, H.A., Gabriel, T.S.J., Hardgrove, C., Mangold, N., Rivera-Hernandez, F., Wiens, R.C., Vasavada, A.R., 2019. An interval of high salinity in ancient Gale crater lake on Mars. *Nat. Geosci.* 12, 889–895.
- Roach, L.H., Mustard, J.F., Murchie, S.L., Bibring, J.-P., Forget, F., Lewis, K.W., Aharonson, O., Vincendon, M., Bishop, J.L., 2009. Testing evidence of recent hydration state change in sulfates on Mars. *J. Geophys. Res. Planets* 114 (E2).
- Robertson, Kevin, Bish, David, 2013. Constraints on the distribution of $\text{CaSO}_4 \cdot n\text{H}_2\text{O}$ phases on Mars and implications for their contribution to the hydrological cycle. *Icarus* 223, 407–417.
- Robertson, K.M., Milliken, R.E., Li, S., 2016. Estimating mineral abundances of clay and gypsum mixtures using radiative transfer models applied to visible-near infrared reflectance spectra. *Icarus* 277, 171–186.
- Savijärvi, H., 1995. Mars boundary layer modeling: diurnal moisture cycle and soil properties at the Viking Lander 1 site. *Icarus* 17, 120–127.
- Schorghofer, Norbert, Aharonson, Oded, 2005. Stability and exchange of subsurface ice on Mars. *J. Geophys. Res. Planets* 110 (E5), E05003. <https://doi.org/10.1029/2004JE002350>.
- Sheppard, Rachel Y., Milliken, Ralph E., Parente, Mario, Itoh, Yuki, 2020. Updated perspectives and hypotheses on the mineralogy of lower Mt. Sharp, Mars, as seen from orbit. *J. Geophys. Res. Planets* 126, e2020JE006372.
- Sheppard, R.Y., Thorpe, M.T., Fraeman, A.A., Fox, V.K., Milliken, R.E., 2021. Merging perspectives on secondary minerals on Mars: a review of ancient water-rock interactions in gale crater inferred from orbital and in-situ observations. *Minerals* 11, 986. <https://doi.org/10.3390/min11090986>.
- Sklute, Elizabeth C., Rogers, A. Deanne, Gregerson, Jason C., Jensen, Heidi B., Reeder, Richard J., Dyar, M. Darby, 2018. Amorphous salts formed from rapid dehydration of multicomponent chloride and ferric sulfate brines: Implications for Mars. *Icarus* 302, 285–295.
- Smith, Rebecca J., Rampe, Elizabeth B., Horgan, Briony H.N., Dehouck, Erwin, 2018. Deriving amorphous component abundance and composition of rocks and sediments on earth and Mars. *J. Geophys. Res. Planets* 123 (10), 2485–2505. <https://doi.org/10.1029/2018JE005612>.
- Smith, R.J., McLennan, S.M., Achilles, C.N., Dehouck, E., Horgan, B.H.N., Mangold, N., et al., 2021. X-Ray amorphous components in sedimentary rocks of Gale crater, Mars: Evidence for ancient formation and long-lived aqueous activity. *J. Geophys. Res. Planets* 126, e2020JE006782. <https://doi.org/10.1029/2020JE006782>.
- Stack, K.M., Milliken, R.E., 2013. Modeling near-infrared reflectance spectra of clay and sulfate mixtures and implications for Mars. *Icarus* 250, 332–356.
- Stack, K.M., Milliken, R.E., 2015. Modeling near-infrared reflectance spectra of clay and sulfate mixtures and implications for Mars. *Icarus* 250, 332–356.
- Stein, N., Grotzinger, J.P., Schieber, J., Mangold, N., Newsom, H., Minitti, M., Sumner, D., Edgett, K.S., Stack, K., Fedo, C., Gupta, S., Hallet, B., Vasavada, A., Fey, D., 2009. Hydrated magnesium sulfates below 0°C – stable phases and polymorphs. In: Abstract at the 40th Lunar and Planetary Science Conference, The Woodlands, TX.
- Sun, Vivian Zheng, 2016. Clays and Opals on Mars: Implications for Water-Rock Interactions Through Time. PhD thesis. Brown University.
- Sutter, A.C. McAdam, Mahaffy, P.R., Ming, D.W., Edgett, K.S., Rampe, E.B., Eigenbrode, J.L., Franz, H.B., Freissinet, C., Grotzinger, J.P., Steele, A., House, C.H., Archer, P.D., Malespin, C.A., Navarro-González, R., Stern, J.C., Bell, J.F., Calef, F.J., Gellert, R., Glavin, D.P., Thompson, L.M., Yen, A.S., 2017. Evolved gas analyses of sedimentary rocks and eolian sediment in Gale Crater, Mars: results of the Curiosity rover's sample analysis at Mars instrument from Yellowknife Bay to the Namib Dune. *J. Geophys. Res. Planets* 122 (12), 2574–2609.
- Tu, V.M., Rampe, E.B., Bristow, T.F., Thorpe, M.T., Clark, J.V., Castle, N., Fraeman, A.A., Edgar, L.A., McAdam, A., Bedford, C., et al., 2021. A review of the phyllosilicates in gale crater as detected by the CheMin instrument on the Mars science laboratory, Curiosity Rover. *Minerals* 11, 847. <https://doi.org/10.3390/min11080847>.
- Turenne, N., Parkinson, A., Applin, D.M., Mann, P., Cloutis, E.A., Mertzman, S.A., 2022. Spectral reflectance properties of minerals exposed to martian surface conditions: Implications for spectroscopy-based mineral detection on Mars. *Planet. Space Sci.* 210, 105377.
- Vaniman, David T., Chipera, Steve J., 2006. Transformations of Mg- and Ca-sulfate hydrates in Mars regolith. *Am. Mineral.* 91, 1628–1642.
- Vaniman, David T., Bish, David L., Chipera, Steve J., Fialips, Claire L., William Carey, J., Feldman, William C., 2004. Magnesium sulphate salts and the history of water on Mars. *Nature* 431, 663–665.
- Vaniman, David T., Martinez, German M., Rampe, Elizabeth B., Bristow, Thomas F., Blake, David F., Yen, Albert S., Ming, Douglas W., Rapin, William, Meslin, Pierre-Yves, Morookian, John Michael, Downs, Robert T., Chipera, Steve J., Morris, Richard V., Morrison, Shaunna M., Treiman, Allan H., Achilles, Cherie N., Robertson, Kevin, Grotzinger, John P., Hazen, Robert M., Wiens, Roger C., Sumner, Dawn Y., 2018. Gypsum, bassanite, and anhydrite at Gale crater, Mars. *Am. Mineral.* 103, 1011–1020.
- Vogels, R., Kerkhoffs, M., Geus, J., 1995. Non-hydrothermal synthesis, characterization and catalytic properties of saponite clays. In: *Studies in Surface Science and Catalysis*. Elsevier, Amsterdam, The Netherlands, pp. 1153–1161.
- Wang, A., Haskin, L.A., Squyres, S.W., Arvidson, R., Jolliff, B.L., Crumpler, L., Gellert, R., Schroder, C., Herkenhoff, K., Hurowitz, J., Tosca, N., Farrand, W., Anderson, R., Knudson, A.T., 2006a. Sulfate deposition in subsurface regolith in Gusev Crater, Mars. *J. Geophys. Res.* 111, E02S17.
- Wang, J.J., Freeman, B.L., Jolliff, I.-M. Chou, 2006b. Sulfates on Mars: a systematic Raman spectroscopic study of hydration states of Mg salts. *Geochim. Cosmochim. Acta.* 70, 6118–6135.
- Wang, Alian, Freeman, J.J., Chou, I-Ming, Jolliff, B.L., 2011. Stability of Mg-sulfates at -10C and the rates of dehydration/rehydration processes under conditions relevant to Mars. *J. Geophys. Res.* 116, E12006.
- Wang, A., Jolliff, B.L., Liu, Y., Connor, K., 2016. Setting constraints on the nature and origin of the two major hydrous sulfates on Mars: monohydrated and polyhydrated sulfates. *J. Geophys. Res. Planets* 121, 678–694. <https://doi.org/10.1002/2015JE004889>.
- Weaver, C.E., 1989. *Clays, Muds and Shales*. Elsevier, New York, NY, USA, p. 810.
- Wilson, Siobhan, Bish, David, 2011. Formation of gypsum and bassanite by cation exchange reactions in the absence of free-liquid H₂O: Implications for Mars. *J. Geophys. Res.* 116, E09010. <https://doi.org/10.1029/2011JE003853>.
- Wilson, Siobhan A., Bish, David L., 2012. Stability of Mg-sulfate minerals in the presence of smectites: possible mineralogical controls on H₂O cycling and biomarker preservation on Mars. *Geochim. Cosmochim. Acta* 96, 120–133.
- Wiseman, S.M., Arvidson, R.E., Wolff, M.J., Smith, M.D., Seelos, F.P., Morgan, F., McGuire, P.C., 2016. Characterization of artifacts introduced by the empirical volcano-scan atmospheric correction commonly applied to CRISM and OMEGA near-infrared spectra. *Icarus* 269, 111–121.